Moment closure approximations of susceptible-infected-susceptible epidemics on adaptive networks

Achterberg, Massimo A.; Van Mieghem, Piet

DOI
10.1103/PhysRevE.106.014308

Publication date
2022

Document Version
Final published version

Published in
Physical review. E

Moment closure approximations of susceptible-infected-susceptible epidemics on adaptive networks

Massimo A. Achterberg* and Piet Van Mieghem
Faculty of Electrical Engineering, Mathematics and Computer Science, Delft University of Technology, P.O. Box 5031, 2600 GA Delft, The Netherlands

(Received 16 February 2022; accepted 29 June 2022; published 25 July 2022)

The influence of people's individual responses to the spread of contagious phenomena, like the COVID-19 pandemic, is still not well understood. We investigate the Markovian Generalized Adaptive Susceptible-Infected-Susceptible (G-ASIS) epidemic model. The G-ASIS model comprises many contagious phenomena on networks, ranging from epidemics and information diffusion to innovation spread and human brain interactions. The connections between nodes in the G-ASIS model change adaptively over time, because nodes make decisions to create or break links based on the health state of their neighbors. Our contribution is fourfold. First, we rigorously derive the first-order and second-order mean-field approximations from the continuous-time Markov chain. Second, we illustrate that the first-order mean-field approximation fails to approximate the epidemic threshold of the Markovian G-ASIS model accurately. Third, we show that the second-order mean-field approximation is a qualitative good approximation of the Markovian G-ASIS model. Finally, we discuss the Adaptive Information Diffusion (AID) model in detail, which is contained in the G-ASIS model. We show that, similar to most other instances of the G-ASIS model, the AID model possesses a unique steady state, but that in the AID model, the convergence time toward the steady state is very large. Our theoretical results are supported by numerical simulations.

DOI: 10.1103/PhysRevE.106.014308

I. INTRODUCTION

A major open problem in epidemiology is to understand the effect of people's personal responses to an epidemic outbreak. For example, an individual can decide to break contact with other individuals to prevent themselves or others from contracting the disease. In that case, the local contact network of the individual is *adapted* by the spread of the disease [1,2]. One of the first adaptive epidemic models was introduced by Gross *et al.* [3], which describes the spread of a susceptible-infected-susceptible (SIS) epidemic on a network. Each node in the network is either infected (I) or healthy but susceptible (S). Each infected node can infect its healthy neighbors with probability p. Independent of the infection process, infected individuals can cure with probability r. To model behavior of individuals, Gross *et al.* introduces a link rewiring process. Susceptible nodes may rewire their link with an infectious neighbor to a randomly chosen susceptible node with probability w. Gross's model was analyzed extensively [4–6] and several other rewiring schemes [7–10] and mean-field methods [11] have been proposed for adaptive SIS epidemics. Link-rewiring schemes have also been investigated in other epidemic models, such as SIR [12] and SIRS models [13].

The seminal work of Gross *et al.* [3] allows for the rewiring of links in the network, but the total number of links in Gross's model is fixed. However, the number of links in the contact network varies over time, especially during an ongoing epidemic. Several studies have considered a time-varying number of links. Tunc *et al.* [14] proposed to break links and automatically restore them after a fixed time. Zhou *et al.* [15] investigated growing networks, in which links between susceptible and infected nodes can be broken. Sahneh *et al.* [16] considered the interplay between the disease spread and the spread of awareness on the disease in a multilayer network. Kiss *et al.* [17] introduced a link activation and deactivation model, also known as the Generalized Adaptive SIS (G-ASIS) model, which was also independently discovered by Achterberg *et al.* [18]. The G-ASIS model assumes that the links between nodes can be changed based on two processes. On the one hand, the link between two nodes can be broken with a certain probability. On the other hand, another rule describes the possibility for a link to be created between two disconnected nodes. The probability for the link-breaking and link-creation processes is dependent on the current health state of the two end-nodes of the link. Hence, the underlying contact network *adapts* to the spread of the epidemic.

Specific instances of the G-ASIS model have been analyzed in detail. The Adaptive SIS (ASIS) model [19,20] describes the spread of an epidemic in a population, where links are broken between susceptible and infected nodes to reduce the spread of the virus and links are recreated between susceptible nodes. The Adaptive Information Diffusion (AID) model, introduced by Trajanovski *et al.* [21], describes the propagation of online content. Taking into account the node's willingness to receive the information, links can be created between susceptible and infected nodes. However, links are removed between susceptible nodes because nodes lose interest in maintaining their relationship when there is no news.

*M.A.Achterberg@tudelft.nl

Several properties of the G-ASIS model have been investigated as well. Kiss *et al.* [17] explored the accuracy of the second-order mean-field approximation of the G-ASIS model, but did not provide any rigorous derivations. Szabó *et al.* [20] provided a detailed bifurcation analysis for the second-order mean-field approximation of the G-ASIS model, but only for the case that links cannot be broken nor created between two infected nodes. Szabó *et al.* additionally proved that the number of steady states is maximally three and derived conditions when such number of steady states exists. A variation on the second-order mean-field approximation of the ASIS model has been studied by Szabó-Solticzky *et al.* [22].

Besides exact lower bounds on the epidemic threshold and implicit solutions for the metastable prevalence [18], no exact results are known for the Markovian G-ASIS model. The Markov chain is a linear process, but the number of states in the Markov chain grows exponentially with the number of nodes. Several methods are known in the literature to approximate exponentially large state spaces. One important method are mean-field approximations, which assume that the states of (groups of) nodes are uncorrelated. Mean-field models were widely popularized in network epidemiology by Pastor-Satorras and Vespignani in 2001, when they illustrated that in scale-free networks, the epidemic threshold converges to zero for infinitely large networks [23]. Ever since, many mean-field methods have been proposed for the static SIS model, including first-order mean-field [24,25] and second-order mean-field approximations [26,27]. The accuracy of the first-order mean-field approximation for the static SIS model has been investigated [28], but the determination of the accuracy of higher order mean-field approximations remains a challenging open problem [29].

Motivated by the mean-field approximations on static SIS networks, we extend the results for adaptive networks. In particular, we discuss the G-ASIS model, in which the links of the underlying graph change based on individual decisions of the nodes. Many properties of the G-ASIS model are hard to compute and approximations are a natural vehicle to gain further understanding of the key epidemiological properties. Here, we present a rigorous derivation of the first-order and second-order mean-field approximations of the G-ASIS model. First, we explicate the G-ASIS model in Sec. II. Section III discusses the first-order mean-field approximation for the G-ASIS model and shows that the first-order mean field fails to mimic the Markovian G-ASIS model. Contrary to the first-order mean field, the second-order mean-field approximation, derived in Sec. IV, is shown to be considerably more accurate. In Sec. V, both first- and second-order mean-field approximations are compared with the Markovian G-ASIS model by numerical simulations. Finally, we present our conclusion and outlook in Sec. VI.

II. THE G-ASIS MODEL

Throughout this work, we use terminology and notation from epidemiology to introduce and explain various concepts, but the results also apply to general spreading phenomena, ranging from gossips, political preferences, opinions, information spread in the human brain, raising awareness about a particular event, innovation spread, cascading failures, and other spreading processes.

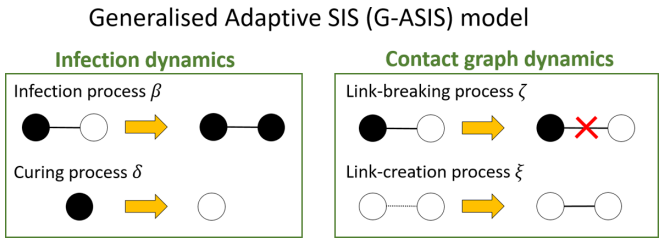

FIG. 1. An overview of the processes in the G-ASIS model. We show a random example for the link-breaking and link-creation mechanisms, where the link is broken between susceptible and infected nodes and is created between two susceptible nodes. All possible updating rules for the link-breaking and link-creation mechanisms are specified in Table I.

We consider a population of N individuals, represented by a graph G where $\mathcal{N}$ is the set of N nodes and $\mathcal{L}$ is the set of L links. Each node represents a particular individual from the population and each link represents the connection between two individuals. The underlying graph G is considered simple, such that the graph G can be represented as an adjacency matrix A, whose elements a_{ij} indicate the existence ($a_{ij} = 1$) or nonexistence ($a_{ij} = 0$) of a link between individuals i and j. We assume that G is undirected, such that the adjacency matrix A is symmetric. We consider a closed population with a fixed number N of individuals (nodes), thus without births and deaths nor migration from or to our population. The "health state" of node i at time t is denoted by the Bernoulli random variable $X_i(t)$, which equals $X_i(t) = 1$ if individual i is infected at time t, and $X_i(t) = 0$ if the individual is healthy, but susceptible. The spread of the epidemic is governed by two processes. Infectious individuals may infect susceptible individuals via a Poisson process with rate β if the two nodes are connected [$a_{ij}(t) = 1$] at time t. Independent of the infection process, infected individuals can cure with Poisson rate δ. The curing process is a nodal process and is not influenced by the network dynamics, in contrast to the infection process that requires a link between an infected and a susceptible node.

The G-ASIS model [18] assumes that the contact graph changes based on two independent processes: link-breaking and link-creation. The link between node i and j at time t is described by the Bernoulli random variable $a_{ij}(t)$. The link a_{ij} between node i and j can be broken with Poisson rate ζ_{ij}. The link-creation process is also a Poisson process with rate ξ_{ij} that creates a link between node i and j. Both the link-breaking and link-creation process are dependent on the health state $X_i(t)$ and $X_j(t)$ of the nodes i and j. One possible example is that links can be created only between susceptible-susceptible pairs and links are broken between susceptible-infected pairs to prevent the spread of the disease. We assume that the infection, curing, link-breaking, and link-creation processes are all independent Poisson processes, whose combined dynamics can be described by a continuous-time Markov chain. Throughout the remainder of this work, we drop the explicit time-dependence of the random variables X_i and a_{ij} for brevity. A schematic overview of the G-ASIS model is shown in Fig. 1.

Most papers on the G-ASIS model so far have assumed that each link in the network changes over time according to the link-breaking and link-creation mechanisms. However, a more general formulation of the G-ASIS model is as follows. We denote the set of permanently nonexisting links in the network by $\mathcal{L}_0$ and the set of permanently existing links by $\mathcal{L}_1$. These links do not adhere to the link-creation and link-breaking mechanisms but instead are nonexistent and always existent, respectively, for all times. The remaining set of links $\mathcal{L}_{\text{adaptive}} = \mathcal{L} \setminus \{\mathcal{L}_0 \cup \mathcal{L}_1\}$ evolve according to the link-creation and link-breaking mechanisms. We denote the number of links of each type by L_0, L_1, and L_{adaptive}, respectively.

The governing equations for the G-ASIS model [18] are

$$\frac{d\,\mathrm{E}[X_i]}{dt} = \mathrm{E}\left[-\delta_i X_i + (1-X_i)\sum_{j=1}^{N}\beta_{ij}X_j a_{ij}\right], \tag{1a}$$

$$\frac{d\,\mathrm{E}[a_{ij}]}{dt} = \begin{cases}\mathrm{E}[-\zeta_{ij}a_{ij}f_{\text{br}}(X_i,X_j) + \xi_{ij}(1-a_{ij})f_{\text{cr}}(X_i,X_j)], & \text{if } (i,j)\in\mathcal{L}_{\text{adaptive}},\\ 0, & \text{otherwise,}\end{cases} \tag{1b}$$

where f_{br} and f_{cr} specify the link-breaking and link-creation process, respectively. All six nontrivial updating rules for the link-breaking f_{br} and link-creation f_{cr} mechanisms have been identified in Ref. [18]. The six updating rules can be written as

$$f(X_i,X_j) = a + b(X_i+X_j) + cX_iX_j, \tag{2}$$

where $a, b, c \in \mathbb{Z}$. The parameters a, b, and c of the six nontrivial updating rules are listed in Table I. Using Eq. (2), the governing equations (1) become

$$\frac{d\,\mathrm{E}[X_i]}{dt} = \mathrm{E}\left[-\delta_i X_i + (1-X_i)\sum_{j=1}^{N}\beta_{ij}X_j a_{ij}\right], \tag{3a}$$

$$\frac{d\,\mathrm{E}[a_{ij}]}{dt} = \begin{cases}\mathrm{E}\{-\zeta_{ij}a_{ij}[a_{\text{br}}+b_{\text{br}}(X_i+X_j)+c_{\text{br}}X_iX_j) + \xi_{ij}(1-a_{ij})(a_{\text{cr}}+b_{\text{cr}}(X_i+X_j)+c_{\text{cr}}X_iX_j]\}, & \text{if } (i,j)\in\mathcal{L}_{\text{adaptive}},\\ 0, & \text{otherwise.}\end{cases} \tag{3b}$$

Equations (3a) and (3b) describe the most general version of the G-ASIS model with heterogeneous infection, curing, link-breaking, and link-creation rates. The fact that some links do not adhere to the link-breaking and link-creation dynamics (that either remain existent or nonexistent for all times) is reflected by the last line of Eq. (3b).

If the link-breaking rate $\zeta_{ij} = 0$ and the link-creation rate $\xi_{ij} = 0$ for all nodes i, j, then the process simplifies to the SIS process on a static network. On the contrary, if $f_{\text{br}} = f_{\text{cr}} = 1$, then the network dynamics is decoupled from the disease dynamics. An extensive analysis for this example of epidemic spreading on temporal networks was provided by Kiss *et al.* [17]. We emphasize that general temporal networks are not necessarily governed by independent link-breaking and link-creation mechanisms, but instead follow more complex patterns, including temporal correlations and cluster formation.

III. FIRST-ORDER MEAN-FIELD APPROXIMATION

Even though the Markovian G-ASIS model (3) is a simple description of spreading processes on adaptive networks, its analysis is difficult. Each of the 36 instances of the G-ASIS model can be described by a Markov chain with $2^{N+L_{\text{adaptive}}}$ states, which makes the computation for any connected graph with more than $N = 20$ nodes infeasible. Only in some special cases, like the adaptive complete graph and the adaptive star graph [30], the huge state space can be reduced using equitable partitions [31].

For all other graphs, the huge state space of the Markov chain can be approximated using mean-field approximations. Mean-field approximations constitute of one or more closure relations, which describe how the higher-order moments of the random variables in the process are approximated by lower-order moments of these random variables [32]. In contrast to the linear Markovian equations, the resulting mean-field equations are nonlinear. Mean-field approximations induce an error, but also significantly reduce the dimensionality of the process [33].

A common mean-field approximation for static networks is the Heterogeneous Mean-Field (HMF) approximation [23], which is a first-order mean-field approximation that additionally considers a topological approximation by aggregating all nodes with the same degree in the same group. The HMF approximation is extended to adaptive networks by Marceau *et al.* [11] for a link rewiring model and by Demirel *et al.* [34] for growing networks. The approximation by Marceau *et al.* not only considers the number of neighbors of each node, but also includes the number of *infected* neighbors in the mean-

TABLE I. All updating rules for the link-breaking and link-creation mechanisms in the G-ASIS model. The table has been adopted from Ref. [18].

Rule f	a	b	c	Gate
X_iX_j	0	0	1	AND
$1-X_iX_j$	1	0	−1	NAND
$(1-X_i)(1-X_j)$	1	−1	1	NOR
$1-(1-X_i)(1-X_j)$	0	1	−1	OR
$(X_i-X_j)^2$	0	1	−2	XOR
$1-(X_i-X_j)^2$	1	−1	2	XNOR

field approximation, thereby improving on the standard HMF approximation. We expect that a similar HMF approximation can be derived for the G-ASIS model using the framework of Devriendt and Van Mieghem [25].

However, the HMF approximation appears inferior [35] to the first-order mean-field approximation without any topological approximation, also known as the N-Intertwined Mean-Field Approximation (NIMFA) [36]. Thus, we focus on NIMFA from here onwards. NIMFA assumes that any pair of random variables X_i, X_j, and a_{ij} is independent (hence, uncorrelated):

$$\mathrm{E}[X_iX_j] = \mathrm{E}[X_i]\mathrm{E}[X_j], \quad \mathrm{E}[X_ia_{ij}] = \mathrm{E}[X_i]\mathrm{E}[a_{ij}],$$
$$\mathrm{E}[X_iX_ja_{ij}] = \mathrm{E}[X_i]\mathrm{E}[X_j]\mathrm{E}[a_{ij}],$$

for all $i \neq j$. The first-order mean-field equations for G-ASIS are then given by

$$\frac{d\,\mathrm{E}[X_i]}{dt} = -\delta_i \mathrm{E}[X_i] + (1-\mathrm{E}[X_i])\sum_{j=1}^{N}\beta_{ij}\mathrm{E}[X_j]\mathrm{E}[a_{ij}], \tag{4a}$$

$$\frac{d\,\mathrm{E}[a_{ij}]}{dt} = \begin{cases} -\zeta_{ij}\mathrm{E}[a_{ij}](a_{\mathrm{br}} + b_{\mathrm{br}}(\mathrm{E}[X_i]+\mathrm{E}[X_j]) + c_{\mathrm{br}}\mathrm{E}[X_i]\mathrm{E}[X_j]) \\ \quad +\xi_{ij}(1-\mathrm{E}[a_{ij}])(a_{\mathrm{cr}} + b_{\mathrm{cr}}(\mathrm{E}[X_i]+\mathrm{E}[X_j]) + c_{\mathrm{cr}}\mathrm{E}[X_i]\mathrm{E}[X_j]), & \text{if } (i,j)\in\mathcal{L}_{\mathrm{adaptive}}, \\ 0. & \text{otherwise.} \end{cases} \tag{4b}$$

Although the number of equations in Eq. (4) is $N + L_{\mathrm{adaptive}}$ and not N, we call Eq. (4) the adaptive N-Intertwined Mean-Field Approximation (aNIMFA), because of the analogy to the NIMFA equations for static networks [36]. Contrary to the NIMFA equations for the static SIS model, aNIMFA is not necessarily an upper bound for the Markovian dynamics.

The steady state of the NIMFA equations and the metastable state of the Markov process show similar behavior for sufficiently large networks and for effective infection rates $\tau = \beta/\delta$ above the epidemic threshold [37]. For adaptive networks, however, we will show that the steady state of the first-order mean-field approximations, like aNIMFA, and the metastable state of the Markov process deviate significantly. One of the reasons is as follows. The curing process in the SIS model only involves the state of the node itself. Any mean-field method will therefore exactly capture the curing process, because the assumed independence of random variables is irrelevant for the curing process. On the contrary, the joint probability of infection of n nodes in network epidemics depends on the joint probabilities of infection of $n+1$ nodes. Any mean-field method, irrespective of its order (smaller than N), will approximate the infection process and induce an approximation error. However, the link-breaking and link-creation processes involve the state of a link plus the states of the adjacent nodes. By using a first-order mean-field approximation, the link-creation and link-breaking processes will be approximated. In Sec. IV, we will construct a second-order mean-field approximation that only involves the approximation of the infection process and exactly captures the link-breaking and link-creation processes.

A. First-order mean field on the complete graph

The inaccuracy of the first-order mean-field approximation is exemplified by the easiest case, in which the infection, curing, link-breaking and link-creation rates are homogeneous parameters and the adaptive graph $\mathcal{L}_{\mathrm{adaptive}}$ is the complete graph, such that $\mathcal{L}_0 = \mathcal{L}_1 = \emptyset$. Then, the aNIMFA equations become

$$\frac{d\,\mathrm{E}[X_i]}{dt} = -\delta\mathrm{E}[X_i] + \beta(1-\mathrm{E}[X_i])\sum_{j=1,j\neq i}^{N}\mathrm{E}[X_j]\mathrm{E}[a_{ij}], \tag{5a}$$

$$\begin{aligned}\frac{d\,\mathrm{E}[a_{ij}]}{dt} &= -\zeta\mathrm{E}[a_{ij}](a_{\mathrm{br}} + b_{\mathrm{br}}(\mathrm{E}[X_i]+\mathrm{E}[X_j]) + c_{\mathrm{br}}\mathrm{E}[X_i]\mathrm{E}[X_j]) \\ &\quad +\xi(1-\mathrm{E}[a_{ij}])(a_{\mathrm{cr}} + b_{\mathrm{cr}}(\mathrm{E}[X_i]+\mathrm{E}[X_j]) + c_{\mathrm{cr}}\mathrm{E}[X_i]\mathrm{E}[X_j]).\end{aligned} \tag{5b}$$

If the initial prevalence is the same for every node and the initial link-density is the same for every link, then Eq. (5) can be simplified. Introducing the average fraction of infected nodes, also known as the prevalence, as $y = \frac{1}{N}\sum_{i=1}^{N}\mathrm{E}[X_i]$, the average link density $z = \frac{1}{N(N-1)}\sum_{i=1}^{N}\sum_{j=1}^{N}\mathrm{E}[a_{ij}]$, rescaling time by $\tilde{t} = t\delta$, defining $\tau = \beta/\delta$, $\tilde{\zeta} = \zeta/\delta$, $\tilde{\xi} = \xi/\delta$ and introducing the normalized effective infection rate $x = \tau(N-1)$, we obtain (dropping the tildes)

$$\frac{d\,y}{dt} = -y + x(1-y)yz, \tag{6a}$$

$$\frac{d\,z}{dt} = -\zeta z(a_{\mathrm{br}} + 2b_{\mathrm{br}}y + c_{\mathrm{br}}y^2) + \xi(1-z)(a_{\mathrm{cr}} + 2b_{\mathrm{cr}}y + c_{\mathrm{cr}}y^2). \tag{6b}$$

After substituting one of the 36 instances of the G-ASIS model, the two differential equations (6) with the parameters τ, ζ, and ξ provide a first-order mean-field description of the G-ASIS model. The steady-state prevalence y_∞ and the steady-state link density z_∞ of Eq. (6) are presented in Theorem III.1.

Theorem III.1. The steady states (y_∞, z_∞) of Eq. (6) are the real-valued solutions of the cubic equation

$$\begin{aligned} &c_{\rm cr}xy_\infty^3 + (2b_{\rm cr}x - c_{\rm cr}x + c_{\rm cr} + c_{\rm br}\omega)y_\infty^2 \\ &\quad + (2b_{\rm cr} + a_{\rm cr}x - 2b_{\rm cr}x + 2b_{\rm br}\omega)y_\infty \\ &\quad + (a_{\rm cr} + a_{\rm br}\omega - a_{\rm cr}x) = 0, \end{aligned} \tag{7}$$

where $\omega = \zeta/\xi$ is the effective link-breaking rate and z_∞ follows as

$$z_\infty = \frac{1}{x(1-y_\infty)} \tag{8}$$

or the steady state equals the trivial (all-healthy) steady state

$$\begin{aligned} &y_\infty = 0 \\ &z_\infty = \begin{cases} \frac{a_{\rm cr}}{a_{\rm br}\omega + a_{\rm cr}}, & \text{if } a_{\rm cr} \neq 0 \text{ or } a_{\rm br} \neq 0, \\ \text{free variable}, & \text{otherwise.} \end{cases} \end{aligned} \tag{9}$$

Proof.

See Appendix A. ∎

Although for $a_{\rm br} = a_{\rm cr} = 0$, there are infinitely many steady states with prevalence $y_\infty = 0$ and link density z_∞, we will continue to call those states the *trivial steady state*, in line with classical SIS epidemics on static networks.

The existence of the trivial steady state $y_\infty = 0$ is illustrated by Theorem III.1. In addition to the trivial steady state, we show in Theorem III.2 that at least one nontrivial steady state exists for all instances in the G-ASIS model.

Theorem III.2. For each instance of the G-ASIS model, there is a nonempty (x, ω)-region where at least one nontrivial steady state exists.

Proof.

See Appendix B. ∎

Theorem III.2 guarantees that the introduction of link-breaking and link-creation mechanisms to the standard SIS model is not able to destroy the endemic state completely. Moreover, the following relation for the epidemic threshold $\tau_c^{(1)}$ follows from the proof of Theorem III.2.

Corollary III.3. For G-ASIS instances whose link-breaking $f_{\rm br}(y)$ and link-creation $f_{\rm cr}(y)$ mechanisms do not have coinciding zeros (see part (ii) in Proof 1 in Appendix B for details), the first-order mean-field epidemic threshold equals

$$\tau_c^{(1)} = \frac{1}{N-1}\frac{a_{\rm cr} + a_{\rm br}\omega}{a_{\rm cr}}.$$

In the sequel, we consider some example instances of the G-ASIS model.

B. The ASIS model

The Adaptive SIS (ASIS) model was introduced by Guo *et al.* [19] to describe the tendency of healthy people to prevent themselves from contracting the disease by avoiding contact with infected individuals. In the ASIS model, links can be broken between susceptible and infected nodes to prevent the disease from spreading and links can be created between susceptible nodes. The link-breaking rule equals $f_{\rm br} = (X_i - X_j)^2$ and the link-creation rule $f_{\rm cr} = (1 - X_i)(1 - X_j)$. Substituting the model parameters of ASIS (see Table I) in Eq. (7) yields

$$\begin{aligned} &xy_\infty^3 + (1 - 3x - 2\omega)y_\infty^2 + (-2 + 3x + 2\omega)y_\infty + (1 - x) \\ &\quad = 0. \end{aligned} \tag{10}$$

The solution $y_\infty = 1$ is not a valid steady state [according to Eq. (6a)] and can be removed. Dividing the polynomial in Eq. (10) by $y_\infty - 1$, reduces to the quadratic equation

$$xy_\infty^2 + (1 - 2x - 2\omega)y_\infty + (x - 1) = 0,$$

whose solutions are

$$y_\infty = 1 - \frac{1-2\omega}{2x} \pm \sqrt{\left(\frac{1-2\omega}{2x}\right)^2 + \frac{2\omega}{x}}. \tag{11}$$

The positive branch of Eq. (11) is infeasible, because y_∞ would be larger than one. For the steady-state solution y_∞ to exist, the expression under the square root in Eq. (11) must be nonnegative and y_∞ must be bounded between zero and one. If one of these criteria is exactly satisfied, thus the expression under the square root is zero or y_∞ is either zero or one, then the resulting condition exactly specifies when the solution y_∞ exists or not. In other words, the existence of y_∞ is described by a bifurcation parameter, also known as the epidemic threshold. Using the relation $x = \tau(N-1)$, the epidemic threshold for the ASIS model follows as

$$\tau_c^{(1),\rm ASIS} = \frac{1}{N-1},$$

and is independent of the effective link-breaking rate ω. To summarize, the solution is

$$y_\infty = \begin{cases} 1 - \frac{1-2\omega}{2\tau(N-1)} - \sqrt{\left[\frac{1-2\omega}{2\tau(N-1)}\right]^2 + \frac{2\omega}{\tau(N-1)}}, & \tau \geqslant \tau_c^{(1),\rm ASIS} = \frac{1}{N-1}, \\ 0, & \text{always.} \end{cases} \tag{12}$$

The steady-state solutions y_∞ are shown for various ω values in Fig. 2. Applying linear stability analysis, we find that the all-healthy state $y_\infty = 0$ is stable for $\tau \leqslant \tau_c$ and is unstable otherwise. If it exists, then the endemic state is always stable.

C. The AID model

The Adaptive Information Diffusion (AID) model was introduced by Trajanovski *et al.* [21] to describe the spread of information. In the AID model, nodes represent people

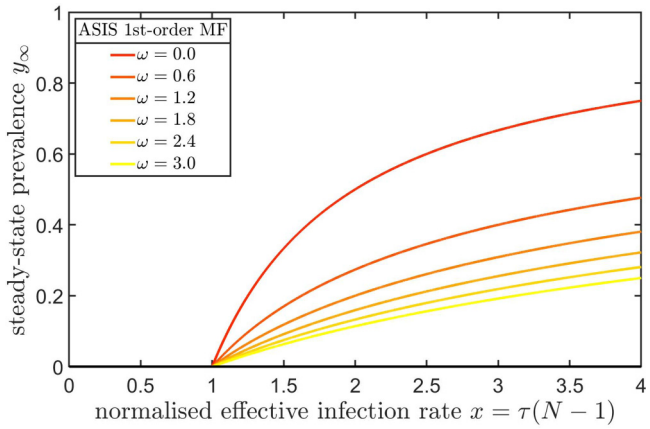

FIG. 2. The transcritical bifurcation in the first-order mean-field ASIS model with $N = 40$ and $\xi = 0.5$. The epidemic threshold τ_c is fixed for varying effective link-breaking rates ω, which contrasts the Markovian ASIS model, where the epidemic threshold τ_c appears to scale linearly with the effective link-breaking rate ω.

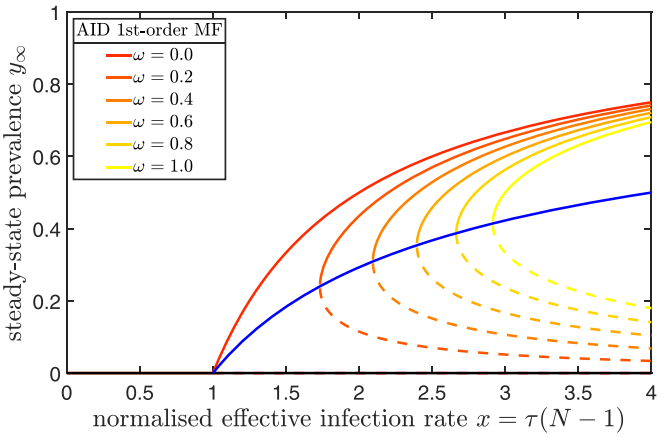

FIG. 3. The saddle-node bifurcation in the first-order mean-field AID model with $N = 40$ and $\xi = 0.5$. The epidemic threshold τ_c moves over the blue line as the effective link-breaking rate ω increases. The Markovian AID model has a nearly constant epidemic threshold τ_c, but the mean-field AID threshold linearly depends on the effective link-breaking rate ω.

who transmit news to their connected neighbors. Links are created between susceptible (informationless) nodes and infected (informative) nodes to enhance the spread of the news. Links are removed between susceptible nodes because both nodes are unaware of the news. The link-breaking rule is $f_{\rm br} = (1 - X_i)(1 - X_j)$ and the link-creation rule $f_{\rm cr} = (X_i - X_j)^2$. Substituting the parameters from the AID model (see Table I) into Eq. (7) yields

$$-2xy_\infty^3 + (4x - 2 + \omega)y_\infty^2 + (2 - 2x - 2\omega)y_\infty + \omega = 0.$$

As before, the solution $y_\infty = 1$ is an invalid steady state. By removing $y_\infty = 1$, the cubic equation simplifies to the quadratic equation

$$2xy_\infty^2 + (-2x + 2 - \omega)y_\infty + \omega = 0,$$

whose solutions are

$$y_\infty = \frac{2x + \omega - 2 \pm \sqrt{(2x + \omega - 2)^2 - 8x\omega}}{4x}. \tag{13}$$

The epidemic threshold τ_c can be determined by checking when the steady-state solution y_∞ is bounded between zero and one and is real-valued. The epidemic threshold follows as

$$\tau_c^{(1),\rm AID} = \frac{\frac{1}{2}(\omega + 2) + \sqrt{2\omega}}{N - 1}. \tag{14}$$

The bifurcation diagram for the AID model is shown in Fig. 3. The main difference between the ASIS and the AID model is that the epidemic threshold in the AID model increases for increasing ω, whereas the epidemic threshold remains constant for the ASIS model. The steady-state solution y_∞ is zero below the epidemic threshold and is nonzero at the epidemic threshold:

$$y_\infty\big(\tau_c^{(1),\rm AID}\big) = \frac{\omega + \sqrt{2\omega}}{\omega + 2 + \sqrt{8\omega}}.$$

To summarize, the solution is

$$y_\infty = \begin{cases} \frac{2\tau(N-1)+\omega-2\pm\sqrt{[2\tau(N-1)+\omega-2]^2-8\tau(N-1)\omega}}{4\tau(N-1)}, & \tau \geqslant \tau_c^{(1),\rm AID} = \frac{\frac{1}{2}(\omega+2)+\sqrt{2\omega}}{N-1}, \\ 0, & \text{always.} \end{cases} \tag{15}$$

The bifurcation diagram in Fig. 3 shows two nontrivial steady states, of which one the upper one is stable and the other is unstable. The stability of each branch was determined using linear stability analysis. The trivial steady state is always stable for the AID model. The existence of the two nontrivial steady states is illustrated in Fig. 4 using varying initial conditions.

An intriguing observation is that the prevalence of the AID model below the epidemic threshold τ_c is zero whereas it is nonzero while approaching the epidemic threshold from above. Similar behavior was, e.g., observed in rewiring models for SIR epidemics [38].

D. The ABN model

The Adaptive Brain Network (ABN) model describes information transport in the human brain [18]. Nodes represent different areas in the human brain and links specify the connections between the brain regions. The nodes can be active (infected) or inactive (healthy). From a control system point of view, the human brain incorporates two brain operational principles: (a) Hebbian learning, where two actively communicating nodes continuously try to improve their communication channel (i.e., increasing the weight of their link, known as their synaptic strength) and (b) homeostatic

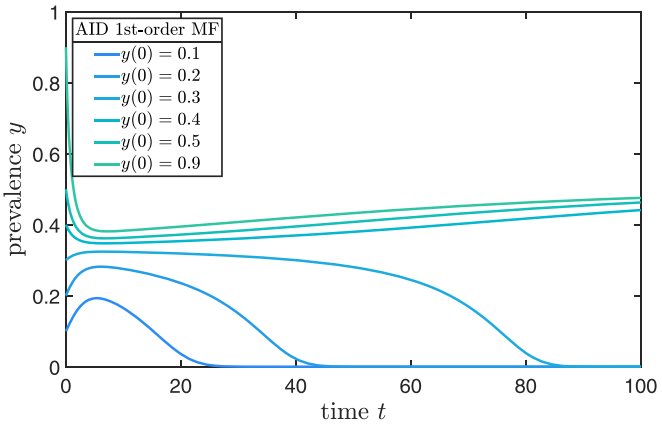

FIG. 4. Numerical solutions of the first-order mean-field AID model using different initial conditions for the fraction of infected nodes, $z(0) = 0.5$, $\xi = \zeta = 0.1$, and $\tau = \frac{3}{N-1}$. As indicated by the bifurcation diagram in Fig. 3, there are two stable steady states: $y_\infty = 0$ and $y_\infty \approx 0.5$. There is also an unstable steady state at $y_\infty \approx 0.35$.

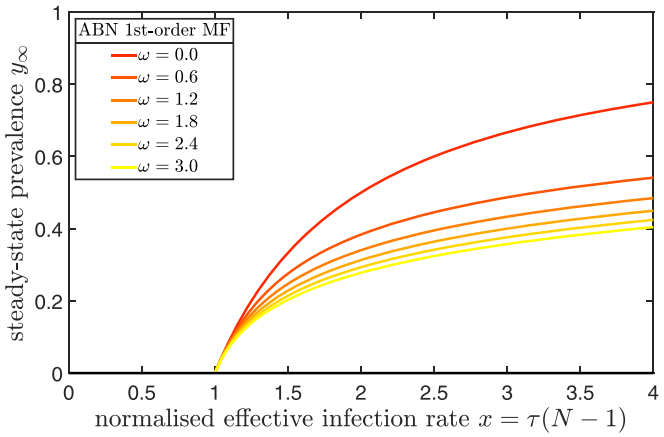

FIG. 5. The transcritical bifurcation in the first-order mean-field ABN model with $N = 40$ and $\xi = 0.5$. The epidemic threshold τ_c remains constant as the effective link-breaking rate ω increases, which is in agreement with the Markovian ABN model.

plasticity [39], which reduces the interaction strength between two connected nodes to prevent a positive coupling generated by Hebbian learning. The ABN model considers homeostatic plasticity to be the primary link-adaptation mechanism. Other G-ASIS instances may be used to describe Hebbian learning.

Thus, the ABN model assumes that links can be created between susceptible (inactive) nodes and links are removed between infected (active) nodes. The link-breaking rule is $f_{\text{br}} = X_i X_j$ and the link-creation rule is $f_{\text{cr}} = (1 - X_i)(1 - X_j)$. Substituting the parameters of the ABN model (see Table I) yields

$$x y_\infty^3 + (1 - 3x + \omega) y_\infty^2 + (3x - 2) y_\infty + (1 - x) = 0. \quad (16)$$

Unfortunately, like many instances of the G-ASIS model, the cubic equation (16) cannot be further simplified. Using Corollary III.3, the epidemic threshold τ_c follows as

$$\tau_c^{(1),\text{ABN}} = \frac{1}{N-1}, \quad (17)$$

which agrees with the numerical results from Fig. 5. The results are similar to the static SIS and ASIS model, which show the existence of a stable endemic steady state above the epidemic threshold. The stability of the all-healthy state changes at the epidemic threshold from stable to unstable, leading to a transcritical bifurcation, as visualized in Fig. 5.

IV. SECOND-ORDER MEAN-FIELD APPROXIMATION

The first-order mean-field approximation, discussed in Sec. III, assumes that any pair of random variables is uncorrelated. In this section, we derive a higher order mean-field approximation, which assumes that pairs, triplets, etc., of random variables are uncorrelated.

Confining ourselves to homogeneous infection, curing, link-breaking, and link-creation rates and all links in the graph adhere to the link-breaking and link-creation mechanisms, the governing equations (3) simplify to

$$\frac{d\,\mathrm{E}[X_i]}{dt} = \mathrm{E}\left[-\delta X_i + \beta(1 - X_i)\sum_{j=1}^{N} X_j a_{ij}\right], \quad (18a)$$

$$\frac{d\,\mathrm{E}[a_{ij}]}{dt} = \mathrm{E}\{-\zeta a_{ij}[a_{\text{br}} + b_{\text{br}}(X_i + X_j) + c_{\text{br}} X_i X_j] + \xi(1 - a_{ij})[a_{\text{cr}} + b_{\text{cr}}(X_i + X_j) + c_{\text{cr}} X_i X_j]\}. \quad (18b)$$

Using the closure relation

$$\mathrm{E}[X_i X_j] \approx \mathrm{E}[X_i]\mathrm{E}[X_j], \quad (19)$$

the following governing equations can be derived (see Appendix C for the derivation)

$$\begin{aligned}
\frac{d\,y}{dt} &= \tau\frac{N-1}{2} z_{\text{SI}} - y,\\
\frac{d\,z_{\text{SS}}}{dt} &= z_{\text{SI}} - \tau(N-2) z_{\text{SSI}} + \xi_{\text{SS}}\left[\frac{N}{N-1}(1-y)^2 - \frac{1}{N-1}(1-y) - z_{\text{SS}}\right] - \zeta_{\text{SS}} z_{\text{SS}},\\
\frac{d\,z_{\text{II}}}{dt} &= \tau z_{\text{SI}} + \tau(N-2) z_{\text{ISI}} - 2 z_{\text{II}} + \xi_{\text{II}}\left(\frac{N}{N-1} y^2 - \frac{1}{N-1} y - z_{\text{II}}\right) - \zeta_{\text{II}} z_{\text{II}},\\
\frac{d\,z_{\text{SI}}}{dt} &= -(1+\tau) z_{\text{SI}} + \tau(N-2) z_{\text{SSI}} - \tau(N-2) z_{\text{ISI}} + 2 z_{\text{II}} + \xi_{\text{SI}}\left[\frac{2N}{N-1} y(1-y) - z_{\text{SI}}\right] - \zeta_{\text{SI}} z_{\text{SI}},
\end{aligned} \quad (20)$$

where y denotes the fraction of infected nodes, z_{SS}, z_{SI}, and z_{II} denote the fraction of links in the graph between susceptible-susceptible (S-S), susceptible-infected (S-I), and infected-infected (I-I) pairs of nodes, respectively. Finally, z_{SSI} and z_{ISI} denote the fraction of connected S-S-I and I-S-I triples in the graph, respectively. Any other triples are irrelevant, because S-S pairs and S-I pairs can only be infected by an external infected node, not by an external susceptible node. The external infected node must be connected to one of the susceptible nodes in the original node pair, leading to the triplet S-S-I or I-S-I.

Many possible closure relations exist, but in Eq. (20), the advantage of our closure relation (19) becomes clear: The unknown variables z_{SSI} and z_{ISI} are related to the infection rate τ only. Using other closure relations than Eq. (19) would lead to an additional approximation of the link-breaking and link-creation processes, which undoubtedly increases the approximation error.

As closure relations for z_{SSI} and z_{ISI}, we use the closure relations from the static SIS model [3,17,26,40], which is derived as follows. We assume that the number of I-S-I triplets equals the number of links between susceptible and infected (S-I) nodes, multiplied by the average number of links between the susceptible node from the considered S-I pair and the remaining infected nodes in the network. The latter equals the number of S-I links divided by the number of susceptible nodes:

$$\frac{1}{2}N(N-1)(N-2)z_{ISI} \approx \frac{1}{2}N(N-1)z_{SI} \cdot \frac{\frac{1}{2}N(N-1)z_{SI}}{N(1-y)}.$$

The same holds for z_{SSI}, except that the infected node can connect to both susceptible nodes of the S-S node pair:

$$\frac{1}{2}N(N-1)(N-2)z_{SSI} \approx \frac{1}{2}N(N-1)z_{SS} \cdot \frac{\frac{1}{2}N(N-1)z_{SI}}{\frac{1}{2}N(1-y)},$$

which can be simplified to

$$z_{ISI} \approx \frac{1}{2}\frac{N-1}{N-2}\frac{z_{SI}^2}{1-y}, \quad z_{SSI} \approx \frac{N-1}{N-2}\frac{z_{SS}z_{SI}}{1-y}. \tag{21}$$

Using the closure relations (21), we obtain a second-order mean-field approximation of the G-ASIS model:

$$\begin{aligned}
\frac{dy}{dt} &= \tau\frac{N-1}{2}z_{SI} - y,\\
\frac{dz_{SS}}{dt} &= z_{SI} - \tau(N-1)\frac{z_{SS}z_{SI}}{1-y} + \xi_{SS}\left[\frac{N}{N-1}(1-y)^2 - \frac{1}{N-1}(1-y) - z_{SS}\right] - \zeta_{SS}z_{SS},\\
\frac{dz_{II}}{dt} &= \tau z_{SI}\left(1 + \frac{N-1}{2}\frac{z_{SI}}{1-y}\right) - 2z_{II} + \xi_{II}\left(\frac{N}{N-1}y^2 - \frac{1}{N-1}y - z_{II}\right) - \zeta_{II}z_{II},\\
\frac{dz_{SI}}{dt} &= -(1+\tau)z_{SI} + \tau(N-1)\frac{z_{SI}}{1-y}\left(z_{SS} - \frac{1}{2}z_{SI}\right) + 2z_{II} + \xi_{SI}\left[\frac{2N}{N-1}y(1-y) - z_{SI}\right] - \zeta_{SI}z_{SI}.
\end{aligned} \tag{22}$$

We would like to intuitively justify Eq. (22), whereby we focus on the equation for the fraction of links between S-S pairs z_{SS}; the other equations follow analogously. The term $\xi_{SS}[\frac{N}{N-1}(1-y)^2 - \frac{1}{N-1}(1-y) - z_{SS}]$ was added for the following reason. The number of S-S links in the network increases with Poisson rate ξ_{SS} based on the number of nonexisting links between pairs of susceptible nodes. Given the number of susceptible nodes $N(1-y)$, the maximum number of S-S links is $\frac{1}{2}[N(1-y)][N(1-y)-1]$. Knowing that the maximum number of links equals $\frac{1}{2}N(N-1)$, the maximum fraction of S-S links equals $\frac{N}{N-1}(1-y)^2 - \frac{1}{N-1}(1-y)$. However, we should subtract the fraction of currently active S-S links, which is given by z_{SS}. Additionally, by breaking S-S links with Poisson rate ζ_{SS}, the number of S-S links should decay exponentially to zero, so we subtract by $\zeta_{SS}z_{SS}$. The other terms are related to the curing and infection process, which we will not explain here.

We derived the second-order mean-field model (22) from the original Markovian model (18) by the following three main steps: (i) we have considered homogeneous parameters and a complete adaptive graph, (ii) we have assumed that the states of any pair of nodes X_i and X_j are independent [see Eq. (19)] and (iii) we have approximated the infection process according to Eq. (21). The variables z_{ISI} and z_{SSI} describe three *connected* I-S-I and S-S-I triplets, consisting of three random variables for the nodal states and two random variables for the intermediate links. Then z_{ISI} and z_{SSI} are approximated in Eq. (21) by z_{SI} and y, which are composed of three and one random variable, respectively. Thus, approximation (iii) is a third-order approximation. At first sight, approximation (ii) in Eq. (19) seems to be a first-order closure relation, because we assume no correlation between any two random variables. However, the states X_i and X_j of the two nodes i and j do not directly influence each other, but can only propagate via the intermediate link a_{ij}, which itself is a stochastic variable. Thus, we argue that (ii) is actually a second-order closure relation. We conclude that our approximation (22) is a second-order *adaptive* mean-field approximation.

A. Second-order mean-field approximations in the literature

Our second-order mean-field approximation (22) is not new, but was introduced by Kiss *et al.* [17] and further analyzed in Refs. [20,22]. Our contribution constitutes of a rigorous derivation of this second-order approximation, starting from the $2^{N+L_{\text{adaptive}}}$ Markov equations (18) toward the second-order mean-field approximation, which we presented

in Appendix C and in the previous subsection. We additionally analyze specific instances of the G-ASIS model in detail by comparing their first- and second-order mean-field approximations.

Our notation for the second-order mean-field equations (22) differs from other notations from the literature [3,17,22]. Most works use $[SS]$, $[II]$, and $[SI]$ to represent (twice) the average number of links between susceptible-susceptible, infected-infected nodes and susceptible-infected nodes, respectively. First, we believe that definitions should be intuitive and should describe the actual number of links; not twice that value. Second, to bring the definitions of z_{SS}, z_{SI}, and z_{II} in line with the definition of the prevalence y, which is the average fraction of infected nodes, we have chosen to normalise all definitions in Eq. (C1) by the maximum number of links, such that z_{SS}, z_{SI} and z_{II} specify the fraction of links rather than the absolute number of links.

Our second-order mean-field approximation (22) is equivalent to the formulation in Kiss *et al.* [17]. This follows by introducing $[I]$ and $[S]$ as the number of infected (susceptible) nodes and $[SS]$ and $[II]$ as twice the number of links between S-S and I-I node pairs, $[SI]$ as the number of S-I links, the link-breaking rate ω, link-creation rate α, curing rate τ, and applying the following transformations to Eqs. (4.1)–(4.4) from Kiss *et al.* [17]:

$$\begin{aligned}
[I] &:= Ny,\\
[S] &:= N(1-y),\\
[SS] &:= N(N-1)z_{\mathrm{SS}},\\
[SI] &:= \frac{1}{2}N(N-1)z_{\mathrm{SI}},\\
[II] &:= N(N-1)z_{\mathrm{II}},\\
\omega_{ab} &:= \zeta_{ab},\\
\alpha_{ab} &:= \xi_{ab},\\
\gamma &:= 1,
\end{aligned}$$

where a, b are any combination of S and I, then we exactly recover the second-order mean-field approximation (22).

A small difference between Ref. [17] and our work is the chosen closure relation. Kiss *et al.* [17] and also Szabó *et al.* [20] consider

$$[ABC] \approx \frac{n-1}{n}\frac{[AB][BC]}{[B]},$$

where A, B, and C are random variables and n is the average number of links per node. We consider the simple case where n is sufficiently large, such that $(n-1)/n \approx 1$.

B. Analysis of the second-order mean field

We proceed our analysis of the second-order mean-field approximation by computing the steady states of Eq. (22).

Theorem IV.1. The steady states of system (22) are the all-healthy state

$$\begin{aligned}
y_\infty = z_{\mathrm{II},\infty} = z_{\mathrm{SI},\infty} &= 0,\\
z_{\mathrm{SS},\infty} &= \begin{cases} \frac{\xi_{\mathrm{SS}}}{\zeta_{\mathrm{SS}}+\xi_{\mathrm{SS}}}, & \text{if } \zeta_{\mathrm{SS}} \neq 0 \text{ or } \xi_{\mathrm{SS}} \neq 0,\\ \text{free variable}, & \text{otherwise,} \end{cases}
\end{aligned} \tag{23}$$

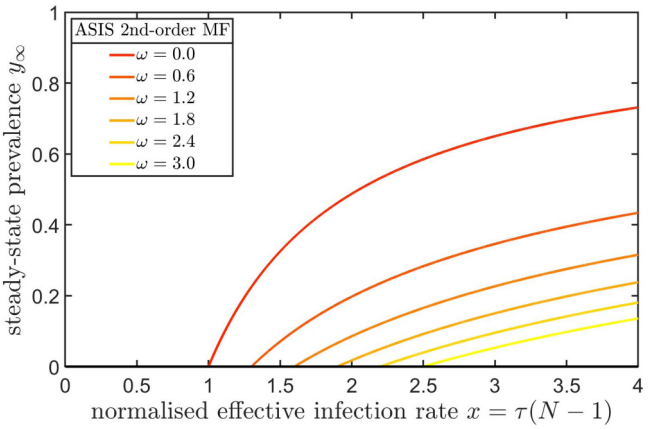

FIG. 6. The transcritical bifurcation in the second-order mean-field ASIS model with $N = 40$ and $\xi = 0.5$. The epidemic threshold τ_c increases linearly with the effective link-breaking rate ω, which is in compliance with the Markov model.

or are the solution of the cubic equation

$$\alpha_1 y_\infty^3 + \alpha_2 y_\infty^2 + \alpha_3 y_\infty + \alpha_4 = 0, \tag{24}$$

where the coefficients $\alpha_1, \alpha_2, \alpha_3$, and α_4 depend on the effective infection rate τ, the link-breaking rate ζ, the link-creation rate ξ, and the choice of the link-breaking and link-creation mechanisms and are given in Eq. (D9) in Appendix D.

Proof.

See Appendix D. ■

Although our model (22) is equivalent to Szabo *et al.* [20], we find a cubic equation (24) for the nontrivial steady states whereas they find a fourth-order equation (see Eq. (11) in Ref. [20]). Actually, the trivial steady state $x = 0$ is a solution of their Eq. (11). After removing $x = 0$, their Eq. (11) simplifies to our Eq. (24).

Equation (23) was obtained earlier for the Markovian G-ASIS model below the epidemic threshold [18] and for the mean-field model in Sec. III. Hence, the all-healthy state from all mean-field approximations is in compliance with the all-healthy state of the Markovian G-ASIS model.

Theorem IV.1 states that the all-healthy state $y_\infty = 0$ corresponds to a steady-state S-S link density $z_{\mathrm{SS},\infty}$, which was earlier reported in Ref. [18, Eq. (9)] and Ref. [20, Eq. (12)] as

$$z_{\mathrm{SS},\infty} = \frac{\xi_{\mathrm{SS}}}{\zeta_{\mathrm{SS}} + \xi_{\mathrm{SS}}}. \tag{25}$$

References [18,20] omitted the case $\zeta_{\mathrm{SS}} = \xi_{\mathrm{SS}} = 0$, which is a viable option (see Table I with all link-updating rules) and the evaluation of $\zeta_{\mathrm{SS}} = \xi_{\mathrm{SS}} = 0$ in Eq. (25) is infeasible. The correct result for the mean-field approximations and the Markov model below the epidemic threshold is reflected by Eq. (23).

Unfortunately, Eq. (24) cannot be further simplified without considering specific link-breaking and link-creation mechanisms. Thus, performing a stability analysis or constructing steady-state solutions is hard for the general case. For the case $\zeta_{\mathrm{II}} = \xi_{\mathrm{II}} = 0$, Szabó *et al.* [20, Theorem 2] derived

a formula for the epidemic threshold:

$$\tau_c = \frac{\zeta_{\text{SI}} + \xi_{\text{SI}} + 1}{(N-1)\frac{\xi_{\text{SS}}}{\xi_{\text{SS}}+\zeta_{\text{SS}}} + N\xi_{\text{SI}}}.$$

For specific instances of the G-ASIS model, we will provide an extensive analysis as follows. We use Maple to analytically compute the steady states of the cubic equation (22) for each of the 36 instances in the G-ASIS model. If the solutions remain very tedious, then we determine the (three) steady states numerically.

C. The ASIS model

We revisit the ASIS model, in which links can be broken between infected-susceptible pairs and links can be created between susceptible nodes. Hence, the link-breaking rule is $f_{\text{br}} = (X_i - X_j)^2$ and the link-creation rule is $f_{\text{cr}} = (1 - X_i)(1 - X_j)$. Or, in the formulation of this section, $\zeta_{\text{SI}} = \zeta$, $\xi_{\text{SS}} = \xi$ and $\zeta_{\text{II}} = \zeta_{\text{SS}} = \xi_{\text{II}} = \xi_{\text{SI}} = 0$. Substituting the model parameters of the ASIS model into Eq. (24), we find

$$(N\tau)y_\infty^3 + (-3N\tau + \tau + \xi\omega + 1 - 2\omega)y_\infty^2 + (3N\tau - 2\tau - 2\xi\omega - 2 - 2\omega)y_\infty + (-N\tau + \tau + \xi\omega + 1) = 0. \tag{26}$$

Equation (26) has $y_\infty = 1$ as a solution, which is an invalid steady state according to Eq. (22). We can remove the solution $y_\infty = 1$ from Eq. (26) to find

$$(N\tau)y_\infty^2 + (-2N\tau + \tau + \xi\omega + 1 - 2\omega)y_\infty + (N\tau - \tau - \xi\omega - 1) = 0,$$

whose solution is

$$y_\infty = 1 - \frac{\tau + 1 + \xi\omega - 2\omega}{2\tau N} \pm \frac{1}{2\tau N}\sqrt{(\tau + 1 + \xi\omega - 2\omega)^2 + 8\tau N\omega}. \tag{27}$$

As before, the solution y_∞ must be real-valued and bounded between zero and one. Then only the negative branch of Eq. (27) appears a valid solution. Moreover, we can derive the epidemic threshold as

$$\tau_c^{(2),\text{ASIS}} = \frac{1 + \xi\omega}{N - 1}. \tag{28}$$

To sum up, we find

$$y_\infty = \begin{cases} 1 - \frac{\tau+1+\xi\omega-2\omega}{2\tau N} - \frac{1}{2\tau N}\sqrt{(\tau + 1 + \xi\omega - 2\omega)^2 + 8\tau N\omega}, & \text{for } \tau \geqslant \tau_c^{(2),\text{ASIS}} = \frac{1+\xi\omega}{N-1}, \\ 0, & \text{always.} \end{cases} \tag{29}$$

For various values of the effective link-breaking rate ω, Fig. 6 shows the bifurcation diagram for the steady-state prevalence y_∞. The epidemic threshold τ_c in Eq. (28) scales linearly in the effective link-breaking rate $\omega = \zeta/\xi$, which is also illustrated in Fig. 6. In contrast to the first-order mean-field threshold $\tau_c^{(1),\text{ASIS}} = \frac{1}{N-1}$, the second-order mean-field threshold $\tau_c^{(2),\text{ASIS}} = \frac{1+\xi\omega}{N-1}$ appears to show the correct linear scaling of the Markovian epidemic threshold [18,19]. Hence, the second-order mean-field approximation is superior to the first-order mean-field approximation for estimating the epidemic threshold τ_c. We further elaborate on this observation in Sec. V.

D. The AID model

As a second example, we revisit the Adaptive Information Diffusion (AID) model. Similar to the ASIS model, we derive the steady states of Eq. (22) by inserting the parameters of the AID model. After the removal of the invalid steady state $y_\infty = 1$, we obtain the following solutions for the steady-state prevalence:

$$y_\infty = \begin{cases} 1 - \frac{2N\tau-\xi\omega+2-\omega\pm\sqrt{(2N\tau+\xi\omega-2+\omega)^2-8N\tau\omega}}{2N\tau(2-\xi\omega)}, & \text{for } 0 < \omega < \omega_c^{\text{AID}} \quad \text{and} \quad \tau \geqslant \tau_c^{(2),\text{AID}}\left(\omega_c^{\text{AID}}\right), \\ 1 - \frac{2N\tau-\xi\omega+2-\omega-\sqrt{(2N\tau+\xi\omega-2+\omega)^2-8N\tau\omega}}{2N\tau(2-\xi\omega)}, & \text{for } \omega \geqslant \omega_c^{\text{AID}} \quad \text{and} \quad \tau > \tau_c^{(2),\text{AID}}, \\ 0, & \text{always,} \end{cases} \tag{30}$$

where we used the effective link-breaking rate $\omega = \zeta/\xi$. We emphasize that $\zeta > 0$ and $\xi > 0$, otherwise the G-ASIS model would not be adaptive. We may compute the epidemic threshold τ_c explicitly in terms of the effective link-breaking rate ω,

$$\tau_c^{(2),\text{AID}}(\omega) = \begin{cases} \frac{1+\frac{\omega}{2}-\frac{\xi\omega}{2}+\sqrt{\omega(2-\xi\omega)}}{N}, & \text{for } 0 < \omega \leqslant \omega_c^{\text{AID}}, \\ \frac{1+\frac{1}{\xi}}{N}, & \text{for } \omega > \omega_c^{\text{AID}}, \end{cases} \tag{31}$$

and the steady-state prevalence y_∞ at the epidemic threshold equals

$$y_\infty\left(\tau = \tau_c^{(2),\text{AID}}\right) = \begin{cases} 1 - \frac{4-2\xi\omega+2\sqrt{\omega(2-\xi\omega)}}{[2+\omega-\xi\omega+2\sqrt{\omega(2-\xi\omega)}](2-\xi\omega)}, & \text{for } 0 < \omega \leqslant \omega_c^{\text{AID}}, \\ 0, & \text{for } \omega > \omega_c^{\text{AID}}. \end{cases} \tag{32}$$

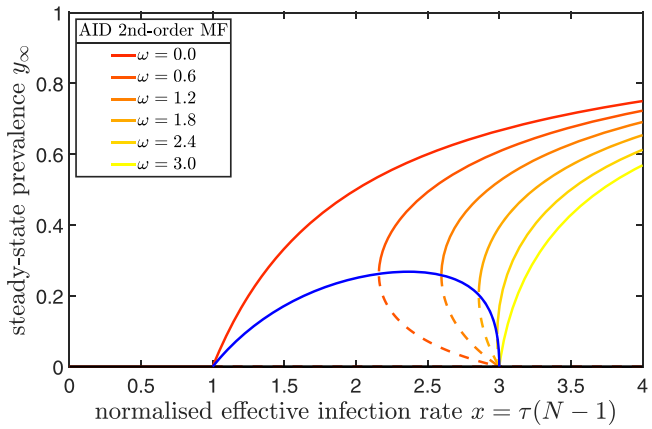

FIG. 7. The bifurcation diagram for the second-order mean-field AID model with $N = 40$ and $\xi = 0.5$. The critical effective link-breaking rate equals $\omega_c^{\mathrm{AID}} = \frac{8}{3} \approx 2.67$. For $0 < \omega \leqslant \omega_c$, there is a saddle-node bifurcation at τ_c and a transcritical bifurcation at $x = 3$. For $\omega > \omega_c$, the bifurcation type is a transcritical. The blue line is a parametric curve from 0 to ω_c, where ω_c is given by Eq. (33).

The critical point ω_c follows by solving $\lim_{\omega\uparrow\omega_c} \tau_c^{(2),\mathrm{AID}}(\omega) = \lim_{\omega\downarrow\omega_c} \tau_c^{(2),\mathrm{AID}}(\omega)$ in Eq. (31), which leads to

$$\omega_c^{\mathrm{AID}}(\xi) = \frac{2}{\xi(\xi+1)}. \tag{33}$$

Figure 7 depicts, as shown by the solution (30), three regions of solutions: (I) For $\omega < \omega_c^{\mathrm{AID}}$ and $\tau < \tau_c^{(2),\mathrm{AID}}$, the only solution is the trivial, all-healthy solution. Then, (II) by applying a fixed $0 < \omega < \omega_c^{\mathrm{AID}}$, there are three solutions for $\tau_c^{(2),\mathrm{AID}} \leqslant \tau \leqslant \tau_c(\omega_c^{\mathrm{AID}})$, of which the upper and lower stable branches are shown in solid lines and the unstable middle branch by dotted lines. Furthermore, there is only one nontrivial stable solution for large infection rates $\tau > \tau_c(\omega_c^{\mathrm{AID}})$. Finally, (III) we consider the case $\omega > \omega_c$. For $\tau \leqslant \tau_c$ the only steady state is the all-healthy state. The location of the epidemic threshold is fixed (in terms of the effective link-breaking rate ω). Above the threshold $\tau > \tau_c$, the only stable steady state is the endemic state. Mostly importantly, the second-order mean-field AID model states that the epidemic threshold $\tau_c^{(2),\mathrm{AID}}$ converges to a constant value while the effective link-breaking rate $\omega \to \infty$. This contrasts the first-order mean-field approximation from Sec. III, where the epidemic threshold τ_c increased up to infinity in the limit of the effective link-breaking rate ω to infinity. Further considerations are given in Sec. V.

The second-order mean-field approximation was primarily derived to gain a deeper understanding of the Markovian G-ASIS model. Trajanovski *et al.* [21] observed spurious oscillations for the Markovian AID model, indicating some kind of instability of the stochastic process. We argue here, albeit hand-waving in nature without providing any rigorous proof, that the metastable state does not fail to exist, but there actually exist two metastable states simultaneously.

Our first reason to believe in the existence of two metastable states, is that the numerical evaluation of the exact, quadratic formula of the prevalence y, provided in Eq. (4) from Ref. [21], reveals that not zero, but two nontrivial solutions y_1 and y_2 exist for the metastable prevalence y. We plot the prevalence y and the computed prevalences y_1 and y_2 in Fig. 8, where y and y_1 overlap nearly perfectly in the metastable state. We emphasize that the computed prevalences y_1 and y_2 are only exact in the metastable state (when all time-derivatives are zero) and not in the transient regime. Our second reason is more technical and is provided in Appendix E.

The behavior before arrival at the steady state is characterized by the bi-metastability phenomenon; the probability to leave the all-healthy state and the endemic state is both very low. Hence, we believe that the two Markovian prevalences y_1 and y_2 from Fig. 8 are similar to the two nontrivial prevalences of the second-order mean-field approximation from Fig. 7, where y_1 corresponds to the stable upper branch and y_2 to the unstable (dashed) lower branch of the second-order mean-field approximation.

Figure 8(a) shows that, starting the process near the endemic state, results in a fast convergence toward the endemic state. Additionally, the infection probability distribution in Fig. 8(b) depicts a bell-shaped curve around $y \approx 0.85$. However, starting with half of the population infected and an empty graph, Fig. 8(c) shows that the convergence toward the endemic state takes a longer time. At $t = 500$, the process from Fig. 8(c) has not yet converged, because the infection probability distribution in Fig. 8(d) is not yet equal to Fig. 8(b).

We provide an example of a much longer convergence time in Fig. 9. Since our simulations involve only $N = 40$ nodes, we believe that for larger networks for some parameter values, the convergence time[1] might be longer than any feasible simulation time. The long convergence times in the AID model contrast the static SIS model and most other instances of the G-ASIS model, whose convergence times are generally much shorter. The consequence is that most AID epidemic outbreaks on large networks never arrive at the metastable state. Hence, the AID model cannot be fully understood from its steady-state distribution alone and research should focus on its time-dependent behavior.

Figure 9(a) additionally shows $y(t) \pm \sigma(t)$, where $\sigma(t)$ is the standard deviation of the prevalence $y(t)$ at time t. The spread around the prevalence y is large, because the time-dependent infection probabilities $\Pr[y = j/N]$, plotted in Fig. 9(b), depicts a composition of two bell-shaped curves; one at $y = 0$ and another at $y \approx 0.7$.

The metastability of the all-healthy state is caused by the link-breaking and link-creation mechanisms of the AID model, which break links between susceptible nodes and create links between susceptible-infected pairs. The all-healthy state corresponds to zero infected nodes and an empty graph. For an outbreak to occur, links must be created and the disease must spread simultaneously, whereas outbreaks in the SIS,

[1]To analyze the exact average convergence time, one possible method is to analyze the eigenvalues of the underlying Markov chain, as was done for ε-SIS dynamics on static networks [41]. Unfortunately, an eigenvalue analysis for the Markovian G-ASIS model is infeasible due to the exponentially large state space, not even for the complete adaptive graph [30].

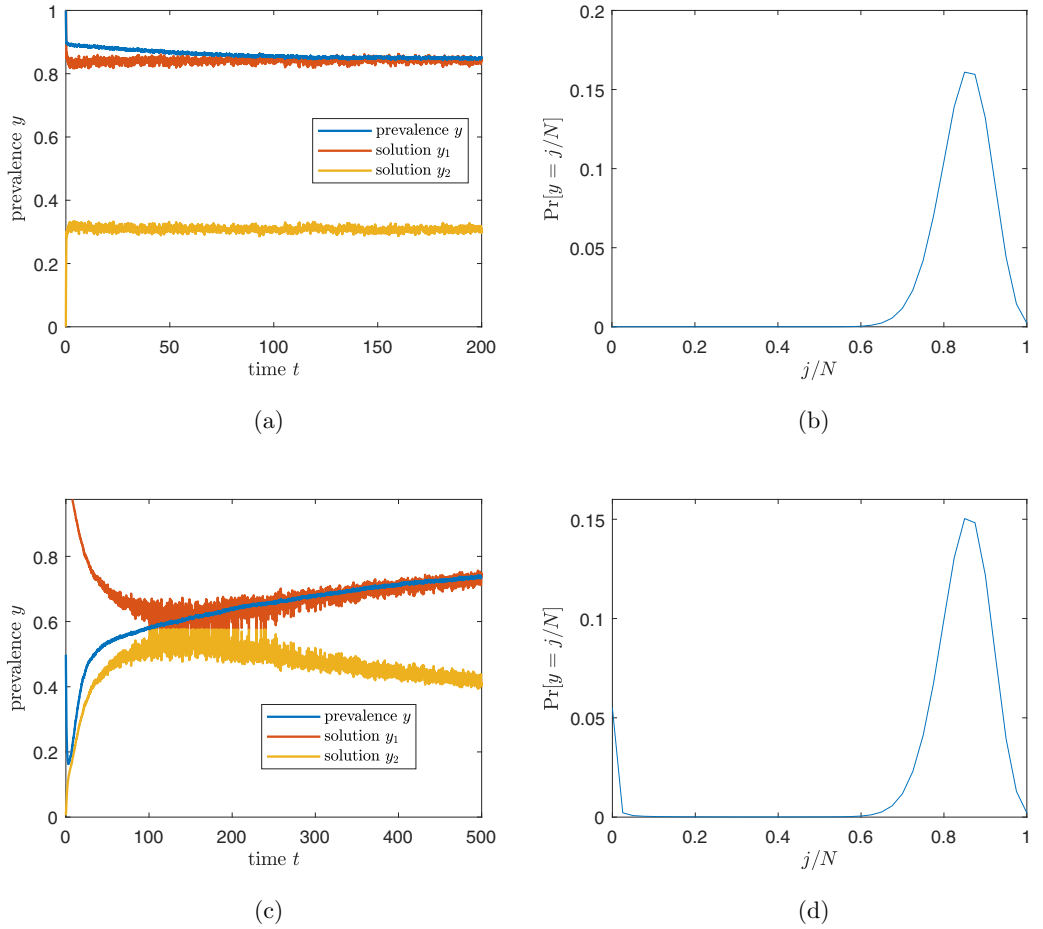

FIG. 8. Illustration of the two metastable states in the AID model with $N = 40$, $\tau = 0.25$, $\zeta = 0.5$, and $\xi = 0.1$ for (a), (c) the time-varying prevalence $y(t)$ and (b), (d) the prevalence distribution $\Pr[y(t) = j/N]$ at time $t = t_{\text{end}}$ where j is the number of infected nodes. The upper plots (a), (b) start with a complete graph and all nodes infected whereas the bottom row (c), (d) initiates with an empty graph and half of the population infected. The results are averaged over 1000 simulations and the computed prevalences y_1 and y_2 are based on the quadratic equation (4) from Ref. [21], but are only exact in the endemic state. We believe that y_1 is stable and y_2 is an unstable solution, analogous to the second-order mean-field solution from Fig. 7. We refer to Sec. V for a description of our simulation method.

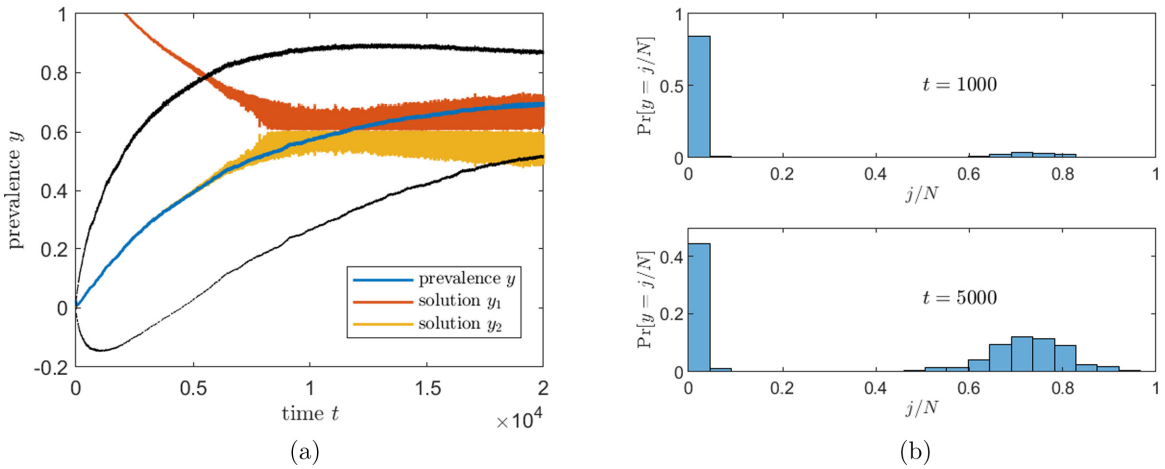

FIG. 9. An example of very long convergence times in the AID model with $N = 40$, $\tau = 0.18$, $\zeta = 0.5$, and $\xi = 0.1$. The simulations are initiated with an empty graph and a single infected node and the results are averaged over 1500 simulations. Subfigure (a) shows the time-dependent prevalence $y(t)$, the computed solutions y_1 and y_2 and the black curves indicate the prevalence $y(t)$ plus/minus one standard deviation $\sigma(t)$. Subfigure (b) shows the prevalence distribution at $t = 1000$ and $t = 5000$.

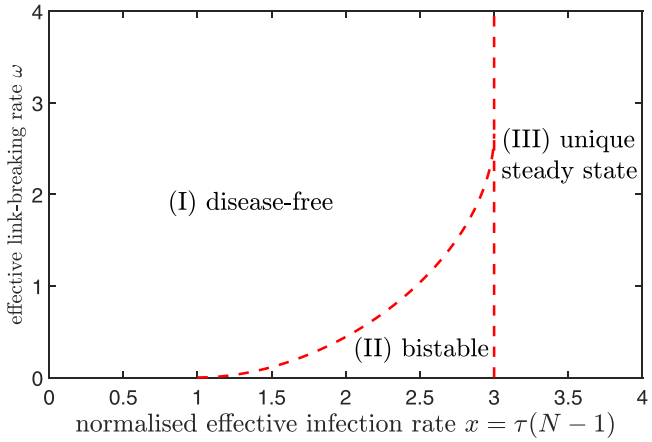

FIG. 10. The phase diagram for the second-order mean-field AID model with $N = 40$ and $\xi = 0.5$. In region (I) only the disease-free state exists, in (III) there exists a unique stable endemic state (and the disease-free state is unstable) and in (II), there are two nontrivial steady states, of which one is stable and the other unstable. The all-healthy state is stable as well.

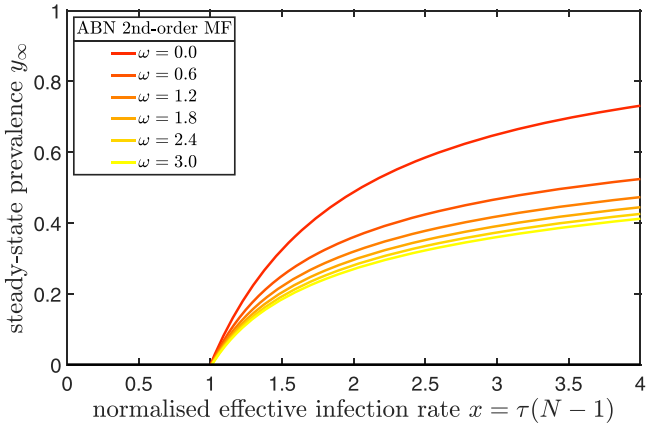

FIG. 11. The transcritical bifurcation in the second-order mean-field ABN model with $N = 40$ and $\xi = 0.5$. The epidemic threshold is constant for varying ω (different lines) but also for changing ξ (not shown).

ASIS, and ABN model are initiated with a single infected node and a completely connected graph, which allows for an easier spread of the disease, because the links already exist in the graph.

We finalize our analysis of the second-order mean-field AID model by showing the phase diagram in Fig. 10. In region (I), the only steady state is the disease-free state. Region (II) is the bistable region, where one endemic state and the all-healthy state are stable and another unstable endemic state exists. In region (III), there is a unique, stable steady state and the all-healthy state is unstable.

E. The ABN model

The steady states of the ABN model satisfy the cubic equation

$$\begin{aligned}&(N\tau\xi\omega + 2N\tau)y_\infty^3 + (-3N\tau\xi\omega - 6N\tau + 2\tau\xi\omega + 2\tau\\ &\quad - 2\tau\omega + 2 + 2\omega)y_\infty^2\\ &\quad + (3N\tau\xi\omega + 6N\tau - 4\tau\xi\omega - 4\tau + 2\tau\omega - \xi\omega - 4)y_\infty\\ &\quad + (-N\tau\xi\omega - 2N\tau + 2\tau\xi\omega + 2\tau + \xi\omega + 2) = 0.\end{aligned}$$

Unfortunately, the cubic equation cannot be further simplified. A numerical approximation of the steady-state prevalence y_∞ is shown in Fig. 11. The epidemic threshold τ_c is approximately located at $\tau_c \approx 1/(N-1)$ for all network sizes N, link-breaking rates ζ, and link-creation rates ξ.

V. NUMERICAL SIMULATIONS

In this section, we compare the Markovian G-ASIS model with the first-order mean-field approximation from Sec. III and second-order mean-field approximation from Sec. IV. We perform many independent Monte Carlo simulations of the Markovian G-ASIS model, whereby we use the sampled-time Markov chain [42] with time step $\Delta t = 0.05$. At each discrete time step, we compute the probability for each node and each link to change its state. If the probability is larger than a random number between zero and one, then the state is changed, and it is left unchanged otherwise. We use a small self-infection rate $\varepsilon = 10^{-3}$ for all simulations [43]. Each simulation starts at $t = 0$ and ends at $t = 500$, unless specified otherwise. The metastable prevalence y is determined by averaging over all simulations and over all prevalences from $t = 100$ to $t = 500$. We focus on the relation between the epidemic threshold τ_c and the effective link-breaking rate ω and illustrate this relation for the ASIS, AID, and ABN model.

The phase diagram for the ASIS model in Fig. 12 illustrates that the static SIS model, shown in blue, has a similar accuracy for both the first-order and second-order mean-field approximation. For the ASIS model, however, the simulations are closer to the second-order mean-field approximation than the first-order mean-field approximation, both in terms of the average distance between the two curves as well as the location of the epidemic threshold. If we estimate the epidemic threshold τ_c from the simulations as the smallest

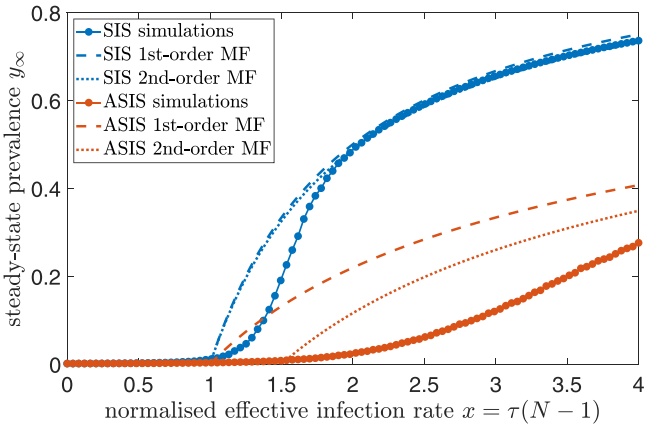

FIG. 12. The phase diagram for the ASIS model on a complete network with $N = 40$ nodes and $\xi = \zeta = 0.5$, $\delta = 1$ for the first and second-order mean-field approximations and the Markovian result is averaged over 1000 simulations.

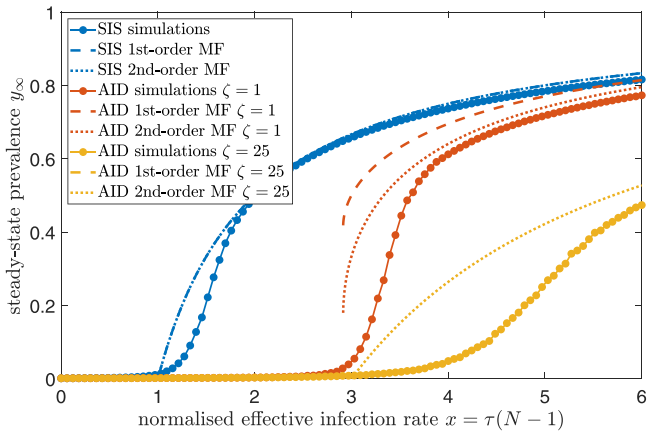

FIG. 13. The phase diagram for the AID model on a complete network with $N = 40$ nodes and $\xi = 0.5, \delta = 1$ for $\zeta = 1$ and $\zeta = 25$ for the first and second order mean-field approximations and the Markovian result is averaged over 1000 simulations. The first-order and second-order mean-field for static SIS are indistinguishable. The first-order mean-field for $\zeta = 25$ is invisible, because the corresponding epidemic threshold is roughly $\tau_c^{(1),\mathrm{AID}} \approx 10/(N-1)$, which is far away from the real threshold at $\tau_c \approx 3/(N-1)$.

effective infection rate τ for which the steady-state prevalence y_∞ exceeds $1/N$, then the estimated threshold τ_c is much closer to the second-order mean-field threshold $\tau_c^{(2),\mathrm{ASIS}}$ than the first-order mean-field threshold $\tau_c^{(1),\mathrm{ASIS}}$.

The phase diagram of the AID model is depicted in Fig. 13. The inaccuracy of the first-order mean-field approximation is large for the AID model. The first-order mean-field approximation predicts a continuously increasing epidemic threshold τ_c, whereas the second-order mean-field approximation predicts a slightly increasing but strictly bounded threshold. The simulations in Fig. 13 show that the epidemic threshold τ_c indeed increases a little, but seems to converge to a finite value for increasing effective link-breaking rates ω.

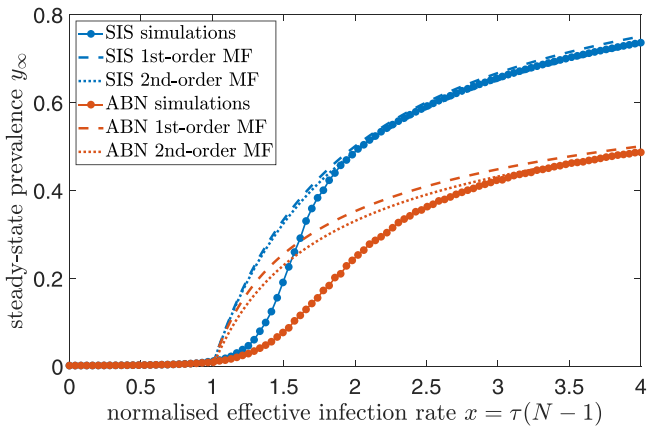

FIG. 14. The phase diagram for the ABN model on a network with $N = 40$ nodes and $\xi = 0.5, \zeta = 0.5, \delta = 1$ for the first and second-order mean-field approximations and the Markovian result is averaged over 1000 simulations.

The situation for the ABN model is plotted in Fig. 14. For the ABN model, both the first-order and second-order mean-field approximation predict a fixed epidemic threshold, which is also exemplified by Fig. 14. In other words, both mean-field approximations capture the epidemic threshold qualitatively correct.

VI. CONCLUSION

In this paper, we have reviewed the Markovian G-ASIS model and considered various mean-field approximations of the Markovian G-ASIS model. We rigorously derived the first-order and second-order mean-field approximations of the G-ASIS model. We discussed two instances of G-ASIS in particular; the Adaptive SIS (ASIS) model where nodes prevent themselves from contracting the disease by breaking connections with infected nodes and the Adaptive Information Diffusion (AID) model that describes the tendency of unaware (healthy) individuals to connect to nodes that are aware (infected) of the gossip or news. We showed that the relation between the epidemic threshold and the effective link-breaking rate is qualitatively captured correctly by the second-order mean-field approximation whereas it is not by the first-order mean-field approximation.

A summary of our results for all possible link-breaking and link-creation updating rules is presented in Table II. For each combination of the link-breaking rule (columns) and link-creation rule (rows), there are three circles. The first circle indicates the scaling of the epidemic threshold in the Markovian model (see Ref. [18] for details). The second and third circle describe the scaling for the first-order mean-field and second-order mean-field approximation, respectively. If the relation is in compliance with the Markovian result, then the circle is green and is red otherwise. If the exact Markovian relation is unknown (reflected by a question mark "?" in the circle), then the circles are orange. In general, Table II confirms that the second-order mean-field approximation better captures the Markovian model than the first-order approximation, although not for all instances of the G-ASIS model.

Finally, we showed that the Markovian AID model was erroneously coined an unstable stochastic model. Instead, we showed that the average convergence time from the all-healthy, empty graph toward the endemic state is very large. The bimetastability phenomenon is in compliance with the second-order mean-field approximation, which also exhibits the bistability phenomenon.

We see several directions for future research. So far, we analyzed 3 of 36 instances of the G-ASIS model in detail, but the remaining models remain largely unexplored. Further investigation on the remaining models, especially those models whose relation between the epidemic threshold and the effective link-breaking rate in Table II remains unclear, may enhance our understanding of the interplay between the disease spreading, network topologies and human decision making. Another underestimated research topic is related to the time-varying graph in adaptive epidemics. Most research focusses on the determination of the number of infected cases, but no or limited attention is devoted to the properties of the underlying network itself. Even though we believe mean-field methods constitute a powerful tool to enhance our under-

TABLE II. All G-ASIS instances and their relation between the epidemic threshold τ_c and the effective link-breaking rate ω. If a circle contains ∞, then τ_c diverges to infinity at a certain finite ω_c. The first circle corresponds to the Markov model (derived in Ref. [18]), the second circle is the first-order mean-field approximation (Sec. III) and the third circle corresponds the second-order mean-field approximation (Sec. IV). Green colored circles indicate a correct approximation, red circles denote incorrect relations and orange circles correspond to undetermined relations. The first-order mean-field approximation predicts 6 correct relations and 9 wrong relations whereas the second-order mean-field approximation predicts 14 correct relations and 1 incorrect relation. Unfortunately, 21 relations have not yet been determined.

Creation \ Breaking	X_iX_j	$1-X_iX_j$	$(1-X_i)(1-X_j)$	$1-(1-X_i)(1-X_j)$	$(X_i-X_j)^2$	$1-(X_i-X_j)^2$
X_iX_j	? ω ∞	? ω ω	? $\sqrt{\omega}$ 1	ω ω ∞	? ω ω	? ω ∞
$1-X_iX_j$	1 1 1	? ω ω	1 ω 1	ω 1 ω	? 1 ω	1 ω 1
$(1-X_i)(1-X_j)$	? 1 1	? ω ω^2	? ω ω	ω 1 ω	? 1 ω	? ω 1
$1-(1-X_i)(1-X_j)$	1 1 1	? ω ω	1 $\sqrt{\omega}$ 1	ω ω ω	? ω ω	1 ω 1
$(X_i-X_j)^2$	1 1 1	? ω ω	1 ω 1	ω ω ω	? ω ω	1 ω 1
$1-(X_i-X_j)^2$	? 1 1	? ω ω	? $\sqrt{\omega}$ 1	ω 1 ω	? 1 ω	? ω 1

standing of Markovian epidemic processes, many properties of the underlying network are not captured by mean-field models, complicating the direct analysis of the underlying, time-varying network.

APPENDIX A: PROOF OF THEOREM III.1

Proof.

The steady states of any dynamical system can be computed by setting the time derivatives to zero. This reduces Eqs. (6a) and (6b) to

$$y_\infty = x(1-y_\infty)y_\infty z_\infty, \tag{A1a}$$

$$\zeta z_\infty\left(a_{\mathrm{br}} + 2b_{\mathrm{br}}y_\infty + c_{\mathrm{br}}y_\infty^2\right) = \xi(1-z_\infty)\left(a_{\mathrm{cr}} + 2b_{\mathrm{cr}}y_\infty + c_{\mathrm{cr}}y_\infty^2\right). \tag{A1b}$$

Equation (A1a) shows that $y_\infty = 0$ is a solution. Inserting $y_\infty = 0$ into Eq. (A1b), we obtain

$$\zeta z_\infty a_{\mathrm{br}} = \xi(1-z_\infty)a_{\mathrm{cr}}.$$

If $a_{\mathrm{cr}} = a_{\mathrm{br}} = 0$, then any value for z_∞ is a steady-state solution. Otherwise, we find

$$z_\infty = \frac{a_{\mathrm{cr}}}{a_{\mathrm{br}}\omega + a_{\mathrm{cr}}}.$$

Now suppose that $y_\infty > 0$, so y_∞ can be removed from Eq. (A1a). Using the effective link-breaking rate $\omega = \zeta/\xi$, Eqs. (A1a) and (A1b) become

$$1 = x(1-y_\infty)z_\infty, \tag{A2a}$$

$$\omega z_\infty\left(a_{\mathrm{br}} + 2b_{\mathrm{br}}y_\infty + c_{\mathrm{br}}y_\infty^2\right) = (1-z_\infty)\left(a_{\mathrm{cr}} + 2b_{\mathrm{cr}}y_\infty + c_{\mathrm{cr}}y_\infty^2\right). \tag{A2b}$$

Equation (A2a) shows that $y_\infty \neq 1$. Before making any further claims about y_∞, we present the following Lemma.

TABLE III. All updating rules in G-ASIS.

Rule f	a	b	c	Quadratic form	Zeros	Gate
X_iX_j	0	0	1	y_∞^2	$y_\infty = 0$ (2x)	AND
$1 - X_iX_j$	1	0	-1	$(1-y_\infty)(1+y_\infty)$	$y_\infty = 1, y_\infty = -1$	NAND
$(1-X_i)(1-X_j)$	1	-1	1	$(1-y_\infty)^2$	$y_\infty = 1$ (2x)	NOR
$1-(1-X_i)(1-X_j)$	0	1	-1	$y_\infty(2-y_\infty)$	$y_\infty = 0, y_\infty = 2$	OR
$(X_i - X_j)^2$	0	1	-2	$2y_\infty(1-y_\infty)$	$y_\infty = 0, y_\infty = 1$	XOR
$1-(X_i - X_j)^2$	1	-1	2	$y_\infty^2 + (1-y_\infty)^2$	$y_\infty \in \mathbb{C}$	XNOR

Lemma A.1. Consider an updating rule f with corresponding parameters a, b, and c from Table III. Then the following function is strictly positive on the interval $0 < y_\infty < 1$:

$$g(y_\infty) = a + 2by_\infty + cy_\infty^2.$$

Proof.

There are six updating rules for the link-creation mechanism $f_{\rm cr}$ and six for the link-breaking mechanism $f_{\rm br}$, which are listed in Table III. Each of these updating rules can be written in a quadratic form. Since $0 < y_\infty < 1$, all quadratic forms are strictly positive. ■

Based on Lemma A.1, we may rewrite Eq. (A2b) in terms of z_∞:

$$z_\infty = \frac{a_{\rm cr} + 2b_{\rm cr}y_\infty + c_{\rm cr}y_\infty^2}{a_{\rm cr} + 2b_{\rm cr}y_\infty + c_{\rm cr}y_\infty^2 + \omega\left(a_{\rm br} + 2b_{\rm br}y_\infty + c_{\rm br}y_\infty^2\right)}. \tag{A3}$$

Substituting Eq. (A3) into Eq. (A2a) gives

$$1 = x(1-y_\infty)\frac{a_{\rm cr} + 2b_{\rm cr}y_\infty + c_{\rm cr}y_\infty^2}{a_{\rm cr} + 2b_{\rm cr}y_\infty + c_{\rm cr}y_\infty^2 + \omega\left(a_{\rm br} + 2b_{\rm br}y_\infty + c_{\rm br}y_\infty^2\right)}. \tag{A4}$$

Rewriting Eq. (A4) gives Eq. (7). ■

APPENDIX B: PROOF OF THEOREM III.2

We present two proofs. The first proof is specifically tailored toward the G-ASIS model and results in Corollary III.3 whereas the second proof is more general and encompasses a larger class of spreading processes.

Proof 1.

We show that Eq. (7) has at least one solution. We split up the proof in two parts.

(i) Consider Eq. (A3) in Appendix A. Equation (7) can be simplified if the zeros of the link-breaking and link-creation mechanisms coincide. Those coinciding zeros are either unphysical (e.g., $y_\infty = -1$ or complex y_∞) or it is redundant (the solution $y_\infty = 0$ was already provided in Theorem III.1) or the solution is invalid [e.g., $y_\infty = 1$, which follows by inserting the solution $y_\infty = 1$ into Eq. (6a)]. The resulting equation is quadratic in y_∞ and can be readily solved. Further working out the details, one can prove that at least one of the solutions is valid in a certain (x, ω) region.

(ii) For the remaining instances without coinciding zeros, we define the function $G(y_\infty)$ as the expression on the left-hand side in Eq. (7). Filling in the two limit cases $y_\infty = 0$ and $y_\infty = 1$, we find

$$G(0) = a_{\rm cr} + a_{\rm br}\omega - a_{\rm cr}x, \quad G(1) = \omega(a_{\rm br} + 2b_{\rm br} + c_{\rm br}) + (a_{\rm cr} + 2b_{\rm cr} + c_{\rm cr}).$$

The expression $G(1)$ is positive, provided that at least one of the two terms is nonzero. The link-creation and link-breaking mechanisms that violate this constraint are actually contained in case (i), thus we may safely assume that $G(1) > 0$. Furthermore, $G(0) < 0$ if

$$a_{\rm cr} + a_{\rm br}\omega < a_{\rm cr}x.$$

The case $a_{\rm cr} = 0$ is contained in case (i), thus we assume $a_{\rm cr} \neq 0$. Thus, we can write

$$x > \frac{a_{\rm cr} + a_{\rm br}\omega}{a_{\rm cr}}. \tag{B1}$$

Equation (B1) describes the condition under which $G(0) < 0$. Given that $G(1) > 0$, the intermediate value theorem states that there must be some $0 < y_\infty < 1$ for which $G(y_\infty) = 0$, which proves the theorem. ■

Proof 2.

We prove Theorem III.2 by showing that the reverse cannot hold, i.e., we look for functions $f_{\rm br}$ and $f_{\rm cr}$ for which no solution exists for all (x, ω) values. We define

$$h(y_\infty) = \omega f_{\rm br}(y_\infty) + f_{\rm cr}(y_\infty) - x(1-y_\infty)f_{\rm cr}(y_\infty),$$

where $f_{\mathrm{br}}(y_\infty)$ is the link-breaking rule and $f_{\mathrm{cr}}(y_\infty)$ is the link-creation rule. If $h(y_\infty) = 0$, then the equation simplifies to Eq. (7). The function h is infinitely differentiable, because h is the composite of such functions f_{br} and f_{cr}. According to the intermediate value theorem, if there exists y_∞ and y'_∞ such that $h(y_\infty) > 0$ and $h(y'_\infty) < 0$, then there must exists some y''_∞ for which holds that $h(y''_\infty) = 0$. To guarantee that solutions do not exist, we must prove that either $h(y_\infty) > 0$ or $h(y_\infty) < 0$ for all y_∞. We focus on the first case, the other case goes analogously. The function f_{cr} is nonnegative and nontrivial (see Table III), thus there must exist some y'_∞ such that $f_{\mathrm{cr}}(y'_\infty) > 0$. To ensure that $h(y'_\infty) > 0$, we find the condition

$$\omega f_{\mathrm{br}}(y'_\infty) + f_{\mathrm{cr}}(y'_\infty) > x(1 - y'_\infty) f_{\mathrm{cr}}(y'_\infty).$$

Suppose $f_{\mathrm{br}}(y'_\infty) = 0$, then the equation simplifies to

$$1 > x(1 - y'_\infty),$$

which is not satisfied unconditionally, that is, for all values of x, except if we would allow $y'_\infty = 1$ as a solution [which is, fortunately, excluded as a steady-state solution, see Eq. (6)]. If $f_{\mathrm{br}}(y'_\infty) > 0$, then the condition can also not be satisfied unconditionally. We conclude that there is always a nonempty (x, ω)-region where at least one solution exists. ■

APPENDIX C: DERIVATION OF THE SECOND-ORDER MEAN-FIELD APPROXIMATION

Prior to the derivation of the second-order mean-field equation, we define the following variables:

$$y = \frac{1}{N}\sum_{i=1}^{N} \mathrm{E}[X_i], \quad z_{\mathrm{ss}} = \frac{1}{N(N-1)}\sum_{i=1}^{N}\sum_{\substack{j=1\\ j\neq i}}^{N} \mathrm{E}[(1-X_i)(1-X_j)a_{ij}],$$

$$z_{\mathrm{si}} = \frac{1}{N(N-1)}\sum_{i=1}^{N}\sum_{\substack{j=1\\ j\neq i}}^{N} \mathrm{E}\{[X_i(1-X_j) + (1-X_i)X_j]a_{ij}\}, \quad z_{\mathrm{ii}} = \frac{1}{N(N-1)}\sum_{i=1}^{N}\sum_{\substack{j=1\\ j\neq i}}^{N} \mathrm{E}[X_i X_j a_{ij}],$$

$$z_{\mathrm{isi}} = \frac{2}{N(N-1)(N-2)}\sum_{i=1}^{N}\sum_{\substack{j=1\\ j\neq i}}^{N}\sum_{\substack{k=1\\ k\neq i\\ k\neq j}}^{N} \mathrm{E}[(1-X_i)X_j X_k a_{ij} a_{ik}],$$

$$z_{\mathrm{ssi}} = \frac{2}{N(N-1)(N-2)}\sum_{i=1}^{N}\sum_{\substack{j=1\\ j\neq i}}^{N}\sum_{\substack{k=1\\ k\neq i\\ k\neq j}}^{N} \mathrm{E}\{[(1-X_i)(1-X_j)X_k + X_i(1-X_j)(1-X_k)]a_{ij}a_{ik}\}, \tag{C1}$$

where y denotes the fraction of infected nodes, z_{ss}, z_{si}, and z_{ii} denote the fraction of links in the graph between susceptible-susceptible (S-S), susceptible-infected (S-I), and infected-infected (I-I) pairs of nodes, respectively. Finally, z_{ssi} and z_{isi} denote the fraction of connected S-S-I and I-S-I triples in the graph, respectively. Any other triples are irrelevant, because S-S pairs and S-I pairs can be infected by an external infected node I. That infected node must be connected to one of the susceptible nodes in the original node pair, leading to the triplet S-S-I or I-S-I.

Using the definitions (C1), the average fraction of links z in the graph is given by

$$z = z_{\mathrm{ss}} + z_{\mathrm{si}} + z_{\mathrm{ii}}. \tag{C2}$$

We derive the governing equation for z_{ii}; the remaining equations can be derived analogously. The governing equation for $\mathrm{E}[X_i X_j a_{ij}]$ is given by

$$\begin{aligned}\frac{d\,\mathrm{E}[X_i X_j a_{ij}]}{dt} = &-2\delta \mathrm{E}[X_i X_j a_{ij}] + \beta \mathrm{E}[(1-X_i)X_j a_{ij}] + \beta \mathrm{E}[X_i(1-X_j)a_{ij}] \\ &+ \beta \sum_{\substack{k=1\\ k\neq i\\ k\neq j}}^{N} \mathrm{E}[(1-X_i)X_j a_{ij} X_k a_{ik}] + \beta \sum_{\substack{k=1\\ k\neq i\\ k\neq j}}^{N} \mathrm{E}[X_i(1-X_j)a_{ij} X_k a_{jk}] \\ &- \zeta_{\mathrm{ii}} \mathrm{E}[X_i X_j a_{ij}] + \xi_{\mathrm{ii}} \mathrm{E}[X_i X_j (1-a_{ij})].\end{aligned} \tag{C3}$$

The G-ASIS model is a Markov chain, where each state encodes which nodes are infected or susceptible and which links are existent or nonexistent in the graph. The possible transitions to and from state $X_i = 1, X_j = 1, a_{ij} = 1$ are as follows: One of the two infected nodes cures [first term on the right-hand side of Eq. (C3)], node j infects node i (second term), node i infects node j (third term), there is an infection from outside (term four and five), the link is broken between node i and node j (term six), or the link is created between node i and node j (term seven) are the possible transitions to and from the state $X_i = 1, X_j = 1, a_{ij} = 1$.

The variable ζ_{II} is defined as $\zeta_{\text{II}} = \zeta(a_{\text{br}} + 2b_{\text{br}} + c_{\text{br}})$ and indicates whether the link can be broken between two infected nodes. Similarly, $\xi_{\text{II}} = \xi(a_{\text{cr}} + 2b_{\text{cr}} + c_{\text{cr}})$ indicates the possibility of a link being created between two infected nodes. Analogously, we define

$$\begin{aligned} &\text{delete S-S link} \quad \zeta_{\text{SS}} = \zeta a_{\text{br}}, && \text{create S-S link} \quad \xi_{\text{SS}} = \xi a_{\text{cr}}, \\ &\text{delete S-I link} \quad \zeta_{\text{SI}} = \zeta(a_{\text{br}} + b_{\text{br}}), && \text{create S-I link} \quad \xi_{\text{SI}} = \xi(a_{\text{cr}} + b_{\text{cr}}), \\ &\text{delete I-I link} \quad \zeta_{\text{II}} = \zeta(a_{\text{br}} + 2b_{\text{br}} + c_{\text{br}}), && \text{create I-I link} \quad \xi_{\text{II}} = \xi(a_{\text{cr}} + 2b_{\text{cr}} + c_{\text{cr}}). \end{aligned}$$

By summing over i and $j \neq i$ in Eq. (C3), multiplying all terms by $\frac{1}{N(N-1)}$ and using the definitions (C1), we find

$$\frac{d\,z_{\text{II}}}{dt} = -2\delta z_{\text{II}} + \beta z_{\text{SI}} + \beta(N-2)z_{\text{ISI}} - \zeta_{\text{II}} z_{\text{II}} - \xi_{\text{II}} z_{\text{II}} + \xi_{\text{II}} \frac{1}{N(N-1)} \sum_{i=1}^{N} \sum_{\substack{j=1 \\ j\neq i}}^{N} \text{E}[X_i X_j].$$

The last term needs to be rewritten as

$$\begin{aligned} \sum_{i=1}^{N} \sum_{\substack{j=1 \\ j\neq i}}^{N} \text{E}[X_i X_j] &= \sum_{i=1}^{N} \sum_{j=1}^{N} \text{E}[X_i X_j] - \sum_{i=1}^{N} \text{E}\big[X_i^2\big] = \sum_{i=1}^{N} \sum_{j=1}^{N} (\text{Cov}[X_i, X_j] + \text{E}[X_i]\text{E}[X_j]) - \sum_{i=1}^{N} \text{E}[X_i] \\ &= \sum_{i=1}^{N} \sum_{j=1}^{N} \text{Cov}[X_i, X_j] + N^2 y^2 - Ny \approx N^2 y^2 - Ny, \end{aligned}$$

where we have made the approximation that the covariance between the state X_i and X_j is zero. Then we finally obtain

$$\frac{d\,z_{\text{II}}}{dt} = -2\delta z_{\text{II}} + \beta z_{\text{SI}} + \beta(N-2)z_{\text{ISI}} - \zeta_{\text{II}} z_{\text{II}} + \xi_{\text{II}} \left(\frac{N}{N-1} y^2 - \frac{1}{N-1} y - z_{\text{II}} \right).$$

Finally, we rescale time $\tilde{t} = \delta t$ and using $\tau = \beta/\delta$, $\tilde{\zeta} = \zeta/\delta$, $\tilde{\xi} = \xi/\delta$, we obtain

$$\frac{d\,z_{\text{II}}}{d\tilde{t}} = -2 z_{\text{II}} + \tau z_{\text{SI}} + \tau(N-2)z_{\text{ISI}} - \tilde{\zeta}_{\text{II}} z_{\text{II}} + \tilde{\xi}_{\text{II}} \left(\frac{N}{N-1} y^2 - \frac{1}{N-1} y - z_{\text{II}} \right).$$

The governing equations for y, z_{SS} and z_{SI} are derived in a similar manner. After dropping the tildes for the time t, link-breaking rate ζ and link-creation rate ξ, we obtain Eq. (20).

APPENDIX D: PROOF OF THEOREM IV.1

Proof.

The steady states of equation (22) are computed by setting the derivatives to zero, such that

$$y_\infty = \tau \frac{N-1}{2} z_{\text{SI},\infty}, \tag{D1a}$$

$$(N-1)\tau \frac{z_{\text{SS},\infty} z_{\text{SI},\infty}}{1-y_\infty} = z_{\text{SI},\infty} + \xi_{\text{SS}} \left[\frac{N}{N-1}(1-y_\infty)^2 - \frac{1}{N-1}(1-y_\infty) - z_{\text{SS},\infty} \right] - \zeta_{\text{SS}} z_{\text{SS},\infty}, \tag{D1b}$$

$$2 z_{\text{II},\infty} = \tau z_{\text{SI},\infty} \left(1 + \frac{N-1}{2} \frac{z_{\text{SI},\infty}}{1-y_\infty} \right) + \xi_{\text{II}} \left(\frac{N}{N-1} y_\infty^2 - \frac{1}{N-1} y_\infty - z_{\text{II},\infty} \right) - \zeta_{\text{II}} z_{\text{II},\infty}, \tag{D1c}$$

$$(1+\tau) z_{\text{SI},\infty} = \tau(N-1) \frac{z_{\text{SI},\infty}}{1-y_\infty} \left(z_{\text{SS},\infty} - \frac{1}{2} z_{\text{SI},\infty} \right) + 2 z_{\text{II},\infty} + \xi_{\text{SI}} \left[\frac{2N}{N-1} y_\infty (1-y_\infty) - z_{\text{SI},\infty} \right] - \zeta_{\text{SI}} z_{\text{SI},\infty}. \tag{D1d}$$

By taking all $z_{\text{II},\infty}$-terms in Eq. (D1c), substituting $z_{\text{II},\infty}$ into Eq. (D1d), we obtain

$$y_\infty = \tau \frac{N-1}{2} z_{\text{SI},\infty} \tag{D2a}$$

$$(N-1)\tau \frac{z_{\text{SS},\infty} z_{\text{SI},\infty}}{1-y_\infty} = z_{\text{SI},\infty} + \xi_{\text{SS}} \left[\frac{N}{N-1}(1-y_\infty)^2 - \frac{1}{N-1}(1-y_\infty) - z_{\text{SS},\infty} \right] - \zeta_{\text{SS}} z_{\text{SS},\infty}, \tag{D2b}$$

$$\begin{aligned} (1+\tau) z_{\text{SI},\infty} = \tau(N-1) \frac{z_{\text{SI},\infty}}{1-y_\infty} \left(z_{\text{SS},\infty} - \frac{1}{2} z_{\text{SI},\infty} \right) + 2 \frac{\tau z_{\text{SI},\infty} \left(1 + \frac{N-1}{2} \frac{z_{\text{SI},\infty}}{1-y_\infty} \right) + \xi_{\text{II}} \left(\frac{N}{N-1} y_\infty^2 - \frac{1}{N-1} y_\infty \right)}{2 + \xi_{\text{II}} + \zeta_{\text{II}}} \\ + \xi_{\text{SI}} \left[\frac{2N}{N-1} y_\infty (1-y_\infty) - z_{\text{SI},\infty} \right] - \zeta_{\text{SI}} z_{\text{SI},\infty}. \end{aligned} \tag{D2c}$$

For readability, we define the positive constant $\alpha_1 = \frac{2}{2+\xi_{\rm II}+\zeta_{\rm II}}$. We substitute Eq. (D2a) into the other equations, such that

$$(N-1)\tau\frac{z_{\rm SS,\infty}z_{\rm SI,\infty}}{1-\tau\frac{N-1}{2}z_{\rm SI,\infty}} = z_{\rm SI,\infty} + \xi_{\rm SS}\left[\frac{N}{N-1}\left(1-\tau\frac{N-1}{2}z_{\rm SI,\infty}\right)^2 - \frac{1}{N-1}\left(1-\tau\frac{N-1}{2}z_{\rm SI,\infty}\right) - z_{\rm SS,\infty}\right] - \zeta_{\rm SS}z_{\rm SS,\infty}, \tag{D3a}$$

$$\begin{aligned}(1+\tau)z_{\rm SI,\infty} &= \tau(N-1)\frac{z_{\rm SI,\infty}}{1-\tau\frac{N-1}{2}z_{\rm SI,\infty}}\left(z_{\rm SS,\infty}-\frac{1}{2}z_{\rm SI,\infty}\right) + \alpha_1\tau z_{\rm SI,\infty}\left(1+\frac{N-1}{2}\frac{z_{\rm SI,\infty}}{1-\tau\frac{N-1}{2}z_{\rm SI,\infty}}\right)\\ &\quad + \alpha_1\xi_{\rm II}\left[\tau^2\frac{N(N-1)}{4}z_{\rm SI,\infty}^2 - \frac{\tau}{2}z_{\rm SI,\infty}\right] + \xi_{\rm SI}\left[\tau N z_{\rm SI,\infty}\left(1-\tau\frac{N-1}{2}z_{\rm SI,\infty}\right) - z_{\rm SI,\infty}\right] - \zeta_{\rm SI}z_{\rm SI,\infty}.\end{aligned} \tag{D3b}$$

One solution of Eq. (D3b) is the all-healthy state $y_\infty = z_{\rm SI,\infty} = z_{\rm II,\infty} = 0$. By inserting the all-healthy state into the original equations (D1), we obtain the steady-state fraction of S-S links $z_{\rm SS,\infty}$ given in the theorem. To remove the all-healthy solution, we divide Eq. (D3b) by $z_{\rm SI,\infty}$, such that

$$(N-1)\tau\frac{z_{\rm SS,\infty}z_{\rm SI,\infty}}{1-\tau\frac{N-1}{2}z_{\rm SI,\infty}} = z_{\rm SI,\infty} + \xi_{\rm SS}\left[\frac{N}{N-1}\left(1-\tau\frac{N-1}{2}z_{\rm SI,\infty}\right)^2 - \frac{1}{N-1}\left(1-\tau\frac{N-1}{2}z_{\rm SI,\infty}\right) - z_{\rm SS,\infty}\right] - \zeta_{\rm SS}z_{\rm SS,\infty}, \tag{D4a}$$

$$\begin{aligned}(1+\tau) &= \tau(N-1)\frac{1}{1-\tau\frac{N-1}{2}z_{\rm SI,\infty}}\left(z_{\rm SS,\infty}-\frac{1}{2}z_{\rm SI,\infty}\right) + \alpha_1\tau\left(1+\frac{N-1}{2}\frac{z_{\rm SI,\infty}}{1-\tau\frac{N-1}{2}z_{\rm SI,\infty}}\right)\\ &\quad + \alpha_1\xi_{\rm II}\left[\tau^2\frac{N(N-1)}{4}z_{\rm SI,\infty} - \frac{\tau}{2}\right] + \xi_{\rm SI}\left[\tau N\left(1-\tau\frac{N-1}{2}z_{\rm SI,\infty}\right) - 1\right] - \zeta_{\rm SI}.\end{aligned} \tag{D4b}$$

Rewriting Eq. (D4a) in terms of $z_{\rm SS,\infty}$ and rearranging Eq. (D4b) while introducing $\alpha_2 = (1+\zeta_{\rm SI}+\xi_{\rm SI}) + (1-\alpha_1+\frac{\alpha_1}{2}\xi_{\rm II} - N\xi_{\rm SI})\tau$, $\alpha_3 = \xi_{\rm SS}+\zeta_{\rm SS}$, we find

$$z_{\rm SS,\infty} = \frac{z_{\rm SI,\infty} + \xi_{\rm SS}\left[\frac{N}{N-1}\left(1-\tau\frac{N-1}{2}z_{\rm SI,\infty}\right)^2 - \frac{1}{N-1}\left(1-\tau\frac{N-1}{2}z_{\rm SI,\infty}\right)\right]}{(N-1)\tau z_{\rm SI,\infty} + \alpha_3\left(1-\tau\frac{N-1}{2}z_{\rm SI,\infty}\right)}\left(1-\tau\frac{N-1}{2}z_{\rm SI,\infty}\right), \tag{D5a}$$

$$\alpha_2 = \tau(N-1)\frac{z_{\rm SS,\infty}}{1-\tau\frac{N-1}{2}z_{\rm SI,\infty}} + (\alpha_1-1)\tau\frac{N-1}{2}\frac{z_{\rm SI,\infty}}{1-\tau\frac{N-1}{2}z_{\rm SI,\infty}} + \frac{\tau^2N(N-1)}{4}(\alpha_1\xi_{\rm II}-2\xi_{\rm SI})z_{\rm SI,\infty}. \tag{D5b}$$

Substituting Eq. (D5a) into Eq. (D5b), we obtain

$$\begin{aligned}\alpha_2 &= \tau(N-1)\frac{\xi_{\rm SS} + \left(\frac{\tau}{2}\xi_{\rm SS} - N\tau\xi_{\rm SS} + 1\right)z_{\rm SI,\infty} + \xi_{\rm SS}\frac{(N-1)^2}{4}\tau^2z_{\rm SI,\infty}^2}{\alpha_3 + \left(1-\frac{1}{2}\alpha_3\right)\tau(N-1)z_{\rm SI,\infty}}\\ &\quad + (\alpha_1-1)\tau\frac{N-1}{2}\frac{z_{\rm SI,\infty}}{1-\tau\frac{N-1}{2}z_{\rm SI,\infty}} + \frac{\tau^2N(N-1)}{4}(\alpha_1\xi_{\rm II}-2\xi_{\rm SI})z_{\rm SI,\infty}.\end{aligned} \tag{D6}$$

Defining $\alpha_4 = (N-1)\tau\xi_{\rm SS}$, $\alpha_5 = \tau(N-1)(\frac{\tau}{2}-N\tau)\xi_{\rm SS} + (N-1)\tau$, $\alpha_6 = \xi_{\rm SS}\frac{(N-1)^3}{4}\tau^3$, $\alpha_7 = \frac{\tau^2N(N-1)}{4}(\alpha_1\xi_{\rm II}-2\xi_{\rm SI})$, and $\alpha_8 = (1-\frac{1}{2}\alpha_3)\tau(N-1)$, we find

$$\alpha_2 = \frac{\alpha_4+\alpha_5z_{\rm SI,\infty}+\alpha_6z_{\rm SI,\infty}^2}{\alpha_3+\alpha_8z_{\rm SI,\infty}} + (\alpha_1-1)\tau\frac{N-1}{2}\frac{z_{\rm SI,\infty}}{1-\tau\frac{N-1}{2}z_{\rm SI,\infty}} + \alpha_7z_{\rm SI,\infty}. \tag{D7}$$

Multiplying Eq. (D7) with $1-\tau\frac{N-1}{2}z_{\rm SI,\infty}$ gives

$$\begin{aligned}\alpha_2 &= \frac{\alpha_4 + \left(\alpha_5 - \tau\frac{N-1}{2}\alpha_4\right)z_{\rm SI,\infty} + \left(\alpha_6 - \tau\frac{N-1}{2}\alpha_5\right)z_{\rm SI,\infty}^2 - \tau\frac{N-1}{2}\alpha_6z_{\rm SI,\infty}^3}{\alpha_3+\alpha_8z_{\rm SI,\infty}}\\ &\quad + \left[\tau\frac{N-1}{2}(\alpha_1-1+\alpha_2)+\alpha_7\right]z_{\rm SI,\infty} - \alpha_7\tau\frac{N-1}{2}z_{\rm SI,\infty}^2.\end{aligned} \tag{D8}$$

Multiplying Eq. (D8) with $\alpha_3+\alpha_8z_{\rm SI,\infty}$ and rearranging, gives us the cubic equation

$$\begin{aligned}0 &= \left(\tau\frac{N-1}{2}\alpha_6 + \alpha_7\alpha_8\tau\frac{N-1}{2}\right)z_{\rm SI,\infty}^3 + \left\{\tau\frac{N-1}{2}\alpha_5 - \alpha_6 - \alpha_8\left[\tau\frac{N-1}{2}(\alpha_1-1+\alpha_2)+\alpha_7\right] + \alpha_3\alpha_7\tau\frac{N-1}{2}\right\}z_{\rm SI,\infty}^2\\ &\quad + \left\{\alpha_2\alpha_8 + \tau\frac{N-1}{2}\alpha_4 - \alpha_5 - \alpha_3\left[\tau\frac{N-1}{2}(\alpha_1-1+\alpha_2)+\alpha_7\right]\right\}z_{\rm SI,\infty} + (\alpha_2\alpha_3-\alpha_4).\end{aligned} \tag{D9}$$

Finally, using the identity $y_\infty = \tau\frac{N-1}{2}z_{\rm SI,\infty}$, we obtain the required cubic equation for y_∞. ■

APPENDIX E: THE TWO METASTABLE STATES IN THE MARKOVIAN AID MODEL

Trajanovski *et al.* [21] proved that the metastable state of the Markovian AID model does not exist if $\mathrm{Var}[Z^*] > 1/4$, where Z^* is the metastable fraction of infected nodes (see Eq. (4) in Ref. [21]). Achterberg *et al.* [18] attempted to prove the instability conjecture in vain (see Conjecture III.1 in Ref. [18]). Here, we make plausible that two metastable states co-exist. One of the reasons is that although $\mathrm{Var}[Z^*] > 1/4$ is a sufficient condition for the nonexistence of the metastable state, Lemma E.1 demonstrates that $\mathrm{Var}[Z^*] > 1/4$ is never satisfied.

Lemma E.1. For the static and adaptive Markovian SIS model, it holds that $\mathrm{Var}[Z^*] < \frac{1}{4}$, where Z^* is the metastable fraction of infected nodes.

Proof.

$$\mathrm{Var}[Z^*] = \mathrm{E}[(Z^*)^2] - \mathrm{E}[Z^*]^2 = \frac{1}{N^2}\mathrm{E}\left[\left(\sum_{i=1}^{N} X_i^*\right)^2\right] - y^2 = \frac{1}{N^2}\mathrm{E}\left[\sum_{i=1}^{N}(X_i^*)^2 + \sum_{i=1}^{N}\sum_{\substack{j=1\\ j\neq i}}^{N} X_i^* X_j^*\right] - y^2$$

$$= \frac{1}{N^2}\mathrm{E}\left[\sum_{i=1}^{N} X_i^*\right] + \frac{1}{N^2}\mathrm{E}\left[\sum_{i=1}^{N}\sum_{\substack{j=1\\ j\neq i}}^{N} X_i^* X_j^*\right] - y^2 = \frac{y}{N} - y^2 + \frac{1}{N^2}\sum_{i=1}^{N}\sum_{\substack{j=1\\ j\neq i}}^{N}\mathrm{E}\left[X_i^* X_j^*\right]$$

$$\overset{\Delta}{\leqslant} \frac{y}{N} - y^2 + \frac{1}{N^2}\sum_{i=1}^{N}\sum_{\substack{j=1\\ j\neq i}}^{N}\mathrm{E}[X_i^*] = \frac{y}{N} - y^2 + \frac{N-1}{N^2}\sum_{i=1}^{N}\mathrm{E}[X_i^*]$$

$$= y(1-y),$$

where the inequality Δ follows from

$$\mathrm{E}[X_i^* X_j^*] = \Pr[X_i^* = 1 \cap X_j^* = 1] = \Pr[X_j^* = 1 | X_i^* = 1]\Pr[X_i^* = 1] \leqslant \Pr[X_i^* = 1] = \mathrm{E}[X_i^*].$$

Since the prevalence y is bounded between zero and one, $\mathrm{Var}[Z^*]$ is bounded between 0 and $\frac{1}{4}$, thus proving our claim. ■

Lemma E.1 proves that the statement $\mathrm{Var}[Z^*] > 1/4$ cannot be satisfied, but does, unfortunately, not guarantee the existence of two metastable states.

The hypothesis in Ref. [21] of the nonexistence of the metastable state and the nonconvergence of the time-varying prevalence $y(t)$ was implicitly based on the assumption of a fast convergence toward the metastable state. Thus, we believe that Fig. 2(b) in Ref. [21] is merely a result of a short simulation period, in which the process has not yet converged to the steady state.

[1] T. Gross and B. Blasius, Adaptive coevolutionary networks: A review, J. R. Soc. Interface. **5**, 259 (2008).

[2] I. B. Schwartz and L. B. Shaw, Rewiring for adaptation, Physics **3**, 17 (2010).

[3] T. Gross, Carlos J. Dommar D'Lima, and B. Blasius, Epidemic Dynamics On an Adaptive Network, Phys. Rev. Lett. **96**, 208701 (2006).

[4] A. Bodó and P. Simon, Analytic study of bifurcations of the pairwise model for SIS epidemic propagation on an adaptive network, Differ. Equ. Dyn. Syst. **28**, 807 (2020).

[5] X. Zhang, C. Shan, Z. Jin, and H. Zhu, Complex dynamics of epidemic models on adaptive networks, J. Diff. Equ. **266**, 803 (2019).

[6] J. Hindes, I. B. Schwartz, and L. B. Shaw, Enhancement of large fluctuations to extinction in adaptive networks, Phys. Rev. E **97**, 012308 (2018).

[7] S. Risau-Gusman and D. H. Zanette, Contact switching as a control strategy for epidemic outbreaks, J. Theor. Biol. **257**, 52 (2009).

[8] T. Britton, D. Juher, and J. Saldaña, A network epidemic model with preventive rewiring: Comparative analysis of the initial phase, Bull. Math. Biol. **78**, 2427 (2016).

[9] N. Sherborne, K. B. Blyuss, and I. Z. Kiss, Bursting endemic bubbles in an adaptive network, Phys. Rev. E **97**, 042306 (2018).

[10] C. Liu, N. Zhou, X. Zhan, G. Sun, and Z. Zhang, Markov-based solution for information diffusion on adaptive social networks, Appl. Math. Comput. **380**, 125286 (2020).

[11] V. Marceau, P.-A. Noël, L. Hébert-Dufresne, A. Allard, and L. J. Dubé, Adaptive networks: Coevolution of disease and topology, Phys. Rev. E **82**, 036116 (2010).

[12] F. Ball, T. Britton, K. Leung, and D. Sirl, A stochastic SIR network epidemic model with preventive dropping of edges, J. Math. Biol. **78**, 1875 (2019).

[13] L. B. Shaw and I. B. Schwartz, Fluctuating epidemics on adaptive networks, Phys. Rev. E **77**, 066101 (2008).

[14] I. Tunc, M. S. Shkarayev, and L. B. Shaw, Epidemics in adaptive social networks with temporary link deactivation, J. Stat. Phys. **151**, 355 (2013).

[15] J. Zhou, G. Xiao, S. A. Cheong, X. Fu, L. Wong, S. Ma, and T. H. Cheng, Epidemic reemergence in adaptive complex networks, Phys. Rev. E **85**, 036107 (2012).
[16] F. D. Sahneh, A. Vajdi, J. Melander, and C. M. Scoglio, Contact adaption during epidemics: A multilayer network formulation approach, IEEE Trans. Netw. Sci. Eng. **6**, 16 (2019).
[17] I. Z. Kiss, L. Berthouze, T. J. Taylor, and P. L. Simon, Modelling approaches for simple dynamic networks and applications to disease transmission models, Proc. R. Soc. A **468**, 1332 (2012).
[18] M. A. Achterberg, J. L. A. Dubbeldam, C. J. Stam, and P. Van Mieghem, Classification of link-breaking and link-creation updating rules in susceptible-infected-susceptible epidemics on adaptive networks, Phys. Rev. E **101**, 052302 (2020).
[19] D. Guo, S. Trajanovski, R. van de Bovenkamp, H. Wang, and P. Van Mieghem, Epidemic threshold and topological structure of susceptible-infectious-susceptible epidemics in adaptive networks, Phys. Rev. E **88**, 042802 (2013).
[20] A. Szabó, P. L. Simon, and I. Z. Kiss, Detailed study of bifurcations in an epidemic model on a dynamic network, Diff. Eq. Appl. **4**, 277 (2012).
[21] S. Trajanovski, D. Guo, and P. Van Mieghem, From epidemics to information propagation: Striking differences in structurally similar adaptive network models, Phys. Rev. E **92**, 030801(R) (2015).
[22] A. Szabó-Solticzky, L. Berthouze, I. Z. Kiss, and P. L. Simon, Oscillating epidemics in a dynamic network model: Stochastic and mean-field analysis, J. Math. Biol. **72**, 1153 (2016).
[23] R. Pastor-Satorras and A. Vespignani, Epidemic Spreading in Scale-Free Networks, Phys. Rev. Lett. **86**, 3200 (2001).
[24] P. Van Mieghem, J. Omic, and R. Kooij, Virus spread in networks, IEEE/ACM Trans. Netw. **17**, 1 (2009).
[25] K. Devriendt and P. Van Mieghem, Unified mean-field framework for susceptible-infected-susceptible epidemics on networks, based on graph partitioning and the isoperimetric inequality, Phys. Rev. E **96**, 052314 (2017).
[26] M. J. Keeling and K. T. D. Eames, Networks and epidemic models, J. R. Soc. Interface. **2**, 295 (2005).
[27] M. Taylor, P. L. Simon, D. M. Green, T. House, and I. Z. Kiss, From Markovian to pairwise epidemic models and the performance of moment closure approximations, J. Math. Biol. **64**, 1021 (2012).
[28] P. Van Mieghem and R. van de Bovenkamp, Accuracy criterion for the mean-field approximation in susceptible-infected-susceptible epidemics on networks, Phys. Rev. E **91**, 032812 (2015).
[29] J. P. Gleeson, S. Melnik, J. A. Ward, M. A. Porter, and P. J. Mucha, Accuracy of mean-field theory for dynamics on real-world networks, Phys. Rev. E **85**, 026106 (2012).
[30] M. A. Achterberg and P. Van Mieghem, An exact reduction of the continuous-time SIS process on adaptive networks is infeasible for most graphs (unpublished).
[31] S. Bonaccorsi, S. Ottaviano, D. Mugnolo, and F. De Pellegrini, Epidemic outbreaks in networks with equitable or almost-equitable partitions, SIAM J. Appl. Math. **75**, 2421 (2015).
[32] C. Kuehn, Moment closure—A brief review, in *Control of Self-organizing Nonlinear Systems* (Springer, Cham, 2016), Chap. 13, pp. 253–271.
[33] F. Darabi Sahneh, C. Scoglio, and P. Van Mieghem, Generalized epidemic mean-field model for spreading processes over multilayer complex networks, IEEE/ACM Trans. Netw. **21**, 1609 (2013).
[34] G. Demirel, E. Barter, and T. Gross, Dynamics of epidemic diseases on a growing adaptive network, Sci. Rep. **7**, 42352 (2017).
[35] C. Li, R. van de Bovenkamp, and P. Van Mieghem, Susceptible-infected-susceptible model: A comparison of n-intertwined and heterogeneous mean-field approximations, Phys. Rev. E **86**, 026116 (2012).
[36] P. Van Mieghem, The N-intertwined SIS epidemic network model, Computing **93**, 147 (2011).
[37] P. Van Mieghem, Universality of the SIS prevalence in networks, arXiv:1612.01386.
[38] F. Ball and T. Britton, Epidemics on networks with preventive rewiring, Random Structures & Algorithms **61**, 250 (2022).
[39] M. Fauth and C. Tetzlaff, Opposing effects of neuronal activity on structural plasticity, Front. Neuroanat. **10**, 75 (2016).
[40] P. Simon, M. Taylor, and I. Kiss, Exact epidemic models on graphs using graph-automorphism driven lumping, J. Math. Biol. **62**, 479 (2011).
[41] M. A. Achterberg, B. Prasse, and P. Van Mieghem, Analysis of continuous-time Markovian ε-SIS epidemics on networks, Phys. Rev. E **105**, 054305 (2022).
[42] P. Van Mieghem, *Performance Analysis of Complex Networks and Systems* (Cambridge University Press, Cambridge, UK, 2014).
[43] P. Van Mieghem and E. Cator, Epidemics in networks with nodal self-infection and the epidemic threshold, Phys. Rev. E **86**, 016116 (2012).